(2)



AD_____

# ENVIRONMENTAL FATE OF NITROGUANIDINE, DIETHYLENEGLYCOL DINITRATE, AND HEXACHLOROETHANE SMOKE

Final Report, Phase II



By

Ronald J. Spanggord
Tsong-Wen Chou
Theodore Mill
Werner Haag
Wyman Lau

September 1987

Supported by

U.S. ARMY MEDICAL RESEARCH AND DEVELOPMENT COMMAND
Fort Detrick, Frederick, Maryland 21701-5012

Contract DAMD17-84-C-4252

SRI Project LSU-7706

SRI International
333 Ravenswood Avenue
Menlo Park, CA 94025

Mr. Mitchell Small, Contracting Officer's Representative
U.S. Army Biomedical Research and Development Laboratory
Fort Detrick, Frederick, Maryland 21701-5010

# REPORT DOCUMENTATION PAGE

| | |
|---|---|
| 1a. REPORT SECURITY CLASSIFICATION<br>UNCLASSIFIED | 1b. RESTRICTIVE MARKINGS |
| 2a. SECURITY CLASSIFICATION AUTHORITY | 3. DISTRIBUTION / AVAILABILITY OF REPORT<br>Approved for public release;<br>Distribution unlimited |
| 2b. DECLASSIFICATION / DOWNGRADING SCHEDULE | |
| 4. PERFORMING ORGANIZATION REPORT NUMBER(S)<br>LSU-7706 | 5. MONITORING ORGANIZATION REPORT NUMBER(S) |
| 6a. NAME OF PERFORMING ORGANIZATION<br>SRI INTERNATIONAL<br>6b. OFFICE SYMBOL (If applicable) | 7a. NAME OF MONITORING ORGANIZATION |
| 6c. ADDRESS (City, State, and ZIP Code)<br>333 Ravenswood Avenue<br>Menlo Park, CA 94025 | 7b. ADDRESS (City, State, and ZIP Code) |
| 8a. NAME OF FUNDING / SPONSORING ORGANIZATION U.S. Army Medical Research & Development Command<br>8b OFFICE SYMBOL (If applicable) | 9. PROCUREMENT INSTRUMENT IDENTIFICATION NUMBER<br>DAMD17-84-C-4252 |
| 8c. ADDRESS (City, State, and ZIP Code)<br>Fort Detrick, Frederick, MD 21701-5012 | 10. SOURCE OF FUNDING NUMBERS<br>PROGRAM ELEMENT NO. 62720A; PROJECT NO 3E1-62720A835; TASK NO. AA; WORK UNIT ACCESSION NO. 015 |

11. TITLE (Include Security Classification)

Environmental Fate of Nitroguanidine, Diethyleneglycol Dinitrate, and Hexachloroethane Smoke

12. PERSONAL AUTHOR(S)

Ronald J. Spanggord, Tsong-Wen Chou, Theodore Mill, Werner Haag, Wyman Lau

| 13a. TYPE OF REPORT | 13b. TIME COVERED | 14. DATE OF REPORT (Year, Month, Day) | 15. PAGE COUNT |
|---|---|---|---|
| Final Report | FROM 5/1/86 TO 4/15/87 | 1987 September 30 | 67 |

16. SUPPLEMENTARY NOTATION

| 17. COSATI CODES | | | 18. SUBJECT TERMS (Continue on reverse if necessary and identify by block number) |
|---|---|---|---|
| FIELD | GROUP | SUB-GROUP | RA 3; photolysis rates, quantum yields, Biotransformation rates. |
| 07 | 02 | | |
| 07 | 03 | | |

19. ABSTRACT (Continue on reverse if necessary and identify by block number)


Nitroguanidine (NG) will photolyze in aqueous systems with a half-life ranging from 0.6 days in summer to 2.3 days in winter. The quantum yield for NG photolysis was measured to be 0.01. NG is initially photolyzed to nitrite and hydroxyguanidine. Hydroxyguanidine undergoes sensitized photolysis to unknown products, and nitrite is photochemically converted to nitrate. NG will biotransform at a rate that is dependent on the concentration of organic nutrients. In the absence of extra organic nutrients, the second-order rate constant was measured to be $3.8 \times 10^{-10}$ ml org$^{-1}$ hr$^{-1}$. No products resulting from biotransformation of NG were observed to buildup in the medium. Cyanamide appears to be an end product of NG utilization.

Diethyleneglycol dinitrate (DEGDN) undergoes aqueous photolysis with a half-life ranging from 15 days in summer to 59 days in winter. The quantum yield for photolysis was


| | |
|---|---|
| 20. DISTRIBUTION / AVAILABILITY OF ABSTRACT<br>☐ UNCLASSIFIED/UNLIMITED ☒ SAME AS RPT. ☐ OTIC USERS | 21. ABSTRACT SECURITY CLASSIFICATION<br>Unclassified |
| 22a NAME OF RESPONSIBLE INDIVIDUAL<br>Mary Frances Bostian | 22b. TELEPHONE (Include Area Code) 301/663-7325<br>22c. OFFICE SYMBOL SGRD-RMI-S |

DD FORM 1473, 84 MAR 83 APR edition may be used until exhausted. All other editions are obsolete.

SECURITY CLASSIFICATION OF THIS PAGE

19. KEY WORDS (Continued)

measured to be 0.18. Photolytic transformation products were identified as 2-hydroxyethylinitratoacetate, nitrate, glycolic acid, and formic acid. DEGDN will biotransform with a second order biotransformation rate constant equal to $3.90 \times 10^{-11}$ ml $org^{-1}$ $hr^{-1}$. A half-life in the New River (Radford, VA) is expected to be 74 days. Polar biotransformation products are produced and do not buildup in the medium.

Hexachloroethane (HCE) will biotransform in the environment with a first-order rate constant of approximately $1.2 \times 10^{-4}$ $hr^{-1}$. The rate of loss will not become significant until organism populations reach $1 \times 10^{8}$ org $ml^{-1}$. The products resulting from biotransformation are tetrachloroethylene and pentachloroethane.

## EXECUTIVE SUMMARY

Nitroguanidine (NG) will photolyze in aqueous systems with half life ranging from 0.6 days in summer to 2.3 days in winter. The quantum yield for NG photolysis was measured to be 0.01. NG is initially photolyzed to nitrite and hydroxyguanidine. Hydroxyguanidine decomposes to ammonia, cyanamide, urea, and guanidine and nitrite is photochemically converted to nitrate. NG will biotransform at a rate that is dependent on the concentration of organic nutrients. In the absence of extra organic nutrients, the second-order rate constant was measured to be $3.8 \times 10^{-10}$ ml $org^{-1}hr^{-1}$. No products resulting from biotransformation of NG were observed to buildup in the medium. Cyanamide appears to be an end product of NG utilization.

Diethyleneglycol dinitrate (DEGDN) undergoes aqueous photolysis with a half-life ranging from 15 days in summer to 59 days in winter. The quantum yield for photolysis was measured to be 0.18. Photolytic transformation products were identified as 2-hydroxyethylnitratoacetate, nitrate, glycolic acid, and formic acid. DEGDN will biotransform with a second order biotransformation rate constant equal to $3.90 \times 10^{-11}$ ml $org^{-1}hr^{-1}$. A half-life in the New River (Radford, VA) is expected to be 74 days. Polar biotransformation products are produced and do not buildup in the medium.

Hexachloroethane (HCE) will biotransform in the environment with a first-order rate constant of approximately $1.2 \times 10^{-4} hr^{-1}$. The rate of loss will not become significant until organism populations reach $1 \times 10^{8}$ org $ml^{-1}$. The products resulting from biotransformation are tetrachloroethylene and pentachloroethane.

## FOREWORD

Citations of commercial organizations and trade names in this report do not constitute an official Department of the Army endorsement or approval of the products or services of these organizations.

CONTENTS

TABLES

FIGURES

# INTRODUCTION

The U.S. Army is responsible for the production of explosives used in conventional military weapons and chemicals used in screening devices to conceal equipment and personnel during military operations. Part of the Army's database to assess the health and environmental impact of such chemicals concerns how long such chemicals persist in the environment and the mechanisms by which their loss and movement is controlled once they are discharged from a manufacturing facility or utilized in training operations.

Three chemicals either being produced or used by the Army are the propellants, nitroguanidine (NG) and diethyleneglycol dinitrate (DEGDN), and hexachloroethane (HCE), a major component of HC smoke. In Phase I (Spanggord et al, 1985), the dominant pathways that control the loss and movement of these chemicals were identified through literature review and laboratory screening studies. These studies identified photolysis as a major transformation route for NG and DEGDN and biotransformation as a major route for HC, NG, and DEGDN. In the studies reported herein, detailed investigations of these processes were undertaken. These investigations include detailed rate studies and the determination of the pseudo-first-order and second-order rate constants for each process. We also investigated transformation products for each process and project their behavior in the environment. These studies serve as an integral part of future studies to model the loss and movement of the test chemicals in the environment.

The studies are reported in five tasks, as follows:

TASK 1. Photochemical Transformation of Nitroguanidine and Identification of Photochemical Transformation Products.

TASK 2. Photochemical Transformation of Diethyleneglycol Dinitrate and Identification of Photochemical Transformation Products.

TASK 3. Biotransformation of Hexachloroethane and Identification of Biotransformation Products.

TASK 4. Biotransformation of Nitroguanidine and Identification of Biotransformation Products.

TASK 5. Biotransformation of Diethyleneglycol Dinitrate and Identification of Biotransformation Products.

## TASK 1

### Photochemical Transformation of Nitroguanidine and Identification of Photochemical Transformation Products

#### Introduction

Nitroguanidine (NG) is a component of a triple-base propellant used in selected artillery rounds. NG is produced at the Sunflower Army Ammunition Plant (SAAP) in DeSoto, Kansas. Most aqueous discharges from this plant are transported by small streams that eventually empty into the Kansas River. Thus, Kansas River (KR) water was chosen as the primary vehicle in which to derive photochemical rate data. The objectives of this task are to determine photochemical products, the first-order photolysis rate constant, $k_p$, and the photochemical quantum yield, $\Phi_c$ of NG. The quantum yield is determined by monitoring the loss of NG as a function of sunlight dose, which is measured by an aqueous p-nitroacetophenone/pyridine (PNAP/PYR) actinometer solution. Details of this methodology have been described by Dulin and Mill (1982). A plot of log [NG] versus log [PNAP] yields a straight line of slope S, from which $\Phi_c$ can be calculated using Equation 1.

$$\Phi_c = \Phi_{PNAP} S \frac{\Sigma \varepsilon_\lambda^{PNAP} L_\lambda}{\Sigma \varepsilon_\lambda^{c} L_\lambda} , \qquad (1)$$

where

$\Phi_{PNAP}$ = quantum yield for the actinometer

$\varepsilon_\lambda^{PNAP}$ = molar absorptivity of PNAP at wavelength $\lambda$

$\varepsilon_\lambda^{c}$ = molar absorptivity of NG at wavelength $\lambda$

$L_\lambda$ = sunlight intensity at wavelength $\lambda$ for a given time of year.

From $\Phi_c$ the first-order photolysis rate constant, $k_p$, can be calculated according to Equation 2 and the half-life, $t_{1/2}$, by Equation 3

$$k_p = \Phi_c \Sigma \varepsilon_\lambda^{c} L_\lambda = S \Phi_{PNAP} \Sigma \varepsilon_\lambda^{PNAP} L_\lambda \qquad (2)$$

$$t_{1/2} = 0.69/k_p \qquad (3)$$

From Equations 1, 2, and 3 it is possible to project the persistence of NG in aqueous systems as a function of the water body and seasonal sunlight intensity.

Since NG has multiple nitrogen atoms in its structure, the potential exists for it to be a charged species in aqueous solution. After careful re-evaluation of the literature on NG ionization (Devries and Gantz, 1954) we have concluded that NG will be present as an uncharged species at environmental pH, rather than in its protonated form, as indicated in our Phase I report. The confusion arises because Devries and Gantz (1954) indicate only that NG has a pKa of 12.1, without specifically stating which ionization step is involved. Subsequent work by Charton (1965) yielded a pKa of 12.8 and assigned it to the equilibrium.

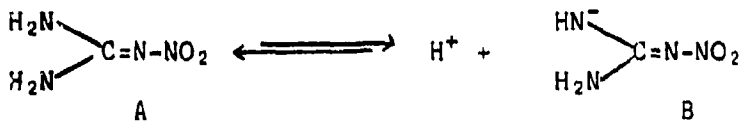

A B

rather than the deprotonation of nitroguanidinium ion. Thus, form A should predominate at pH<12.

## Materials and Methods

NG was obtained from Aldrich Chemical Co. (Lot No. 2029JJ) and contained 25% water as a stabilizer. The NG was oven-dried at 120°C overnight. All other materials were reagent grade or better and were oven-dried when necessary. Nitrite and nitrate were used as their sodium salts, guanidine as its nitrate or acetate salt, and hydroxyguanidine as its sulfate salt.

Kansas River water was obtained near the SAAP. It had an absorbance of 0.039 $cm^{-1}$ at 313 nm. Humic acid solution (HS) was prepared by extracting humic acid (Aldrich Chemical Co.) into water at pH 10 for several days and then adjusting the pH to 7 with phosphoric acid. Experiments with HS were run at 60 mg/l humic acid (TOC=24 mg/l), having an absorbance of 0.66 $cm^{-1}$ at 313 nm. Experiments in distilled water (DW) were run with 5mM phosphate buffer giving a final pH of 7.8, the natural pH of KR water. Both KR water and HS water were filter-sterilized (pore size, 0.2 µm) upon collection or preparation, stored at 3°C, and filtered again (0.45 µm) immediately before use. Experiments were conducted in KR water and HS water, in addition to distilled water, to test for possible sensitization by natural organic and inorganic compounds (Haag and Haighe, 1985, 1986).

Photolyses were performed in sunlight in quartz tubes (1 cm o.d.) held on a rack at 30° from the horizon. The sunlight flux was monitored using PNAP/PYR actinometers. At each time point, actinometer and NG tubes were removed and stored at 3°C in the dark until analysis at the end of the run. A single tube was collected per time point, approximately once per day from 16 to 22 May, 1986. The entire procedure was repeated on 21 to 24 July, 1986. For kinetic runs, the initial NG concentration was 50 µM. For product analyses, 1 mM NG solutions were photolyzed in 50-ml pyrex volumetric flasks on 1 to 5 Aug., 1986.

The loss of NG was monitored by high-performance liquid chromatography (HPLC) using a Hewlett-Packard 1090 liquid chromatograph, a $C_{18}$ 6-cm, 3µm reverse-phase column, water as the mobile phase at 0.4 mL/min, and ultraviolet (UV) detection at 264 nm. The PNAP actinometer solution was monitored with the same column, a mobile phase consisting of 50% acetonitrile in water, and

UV detection at 275 nm. The quantum yield for the actinometer was adjusted by varying the pyridine concentration to yield a half-life similar to that of the compound of interest (Dulin and Mill, 1982).

Nitrite photolyses were performed at an initial concentration of 50 μm in the presence of 2mM pH7 phosphate buffer and two organic scavengers for OH, namely, 1mM pentanol and 10 mg/L HS. A lower concentration of HS was used here compared to NG photolyses to avoid inhibition by light screening. Irradiations were carried out in quartz tubes in sunlight in the same manner as NG irradiations but without actinometry. Actinometry was not necessary because the long exposure periods caused an averaging of the day-night light intensity variations, and because no attempt was made to determine quantum yields. Runs were performed in summer (15 to 29 Aug. 1986), taking samples every 5 days, and in fall (23 Oct. to 22 Nov. 1986), taking samples about every 7 days.

Loss of nitrite and formation of nitrate was determined by ion chromatography using a Dionex 2000; ion chromatograph, an AS4A anion exchange column, 2.2mM $Na_2CO_3$/0.75mM $NaHCO_3$ as the mobile phase, and conductivity detection.

Additional product studies were performed in the laboratory using a 350-watt xenon sunlamp. The lamp has an intensity at 309-400nm about 3 times that of noon summer sunlight at 38°N, as determined by PNAP/PYR actinometry (Dulin and Mill, 1982), allowing more rapid photolysis and a better chance at detecting photolytically produced intermediates which might decay by thermal processes during long experiments. The lamp has a spectral output closely approximating that of sunlight and samples were irradiated in borosilicate (kimax) glass tubes to remove light below 290 nm. Tubes were held stationary, 30 cm in front of the lamp, and kept at room temperature (25±2°C) by use of a fan. Photolyses were carried out on both NG and hydroxyguanidine (an intermediate photolysis product; see below) at initial concentrations of 50 μM. Single samples were pipetted from the tubes into HPLC vials at regular intervals and placed in the dark until analysis. Samples were analyzed for NG, hydroxyguanidine, guanidine, and cyanamide on a 10-cm, 3 μm $C_{18}$ reverse-phase column using 10mM pentanesulfonic acid/1mM $H_2SO_4$ eluent at 2.0 mL/min and UV detection at 190 nm.

Hydroxylamine was determined by the method of Berg and Becker (1940). One-mL aqueous samples were mixed with 1 mL 1% 8-hydroxyquinoline in ethanol and with 1 mL 1.0M sodium carbonate, and incubated at 60°C for 10 minutes. After cooling, absorbance was measured at 710 nm. The detection limit was about 0.5 μM. Absorption spectra were obtained in 1-cm cells on an HP8450A spectrophotometer. Two solutions (in water) were analyzed and the molar absorptivities averaged.

## Photolysis Results

The UV absorption spectrum of NG appears in Figure 1. The molar absorptivity ($\varepsilon_\lambda$) at various wavelengths above 297.5 nm, the light intensity for spring and summer months ($L_\lambda$), and the product of $\varepsilon_\lambda L_\lambda$ for spring and summer are presented in Table 1.

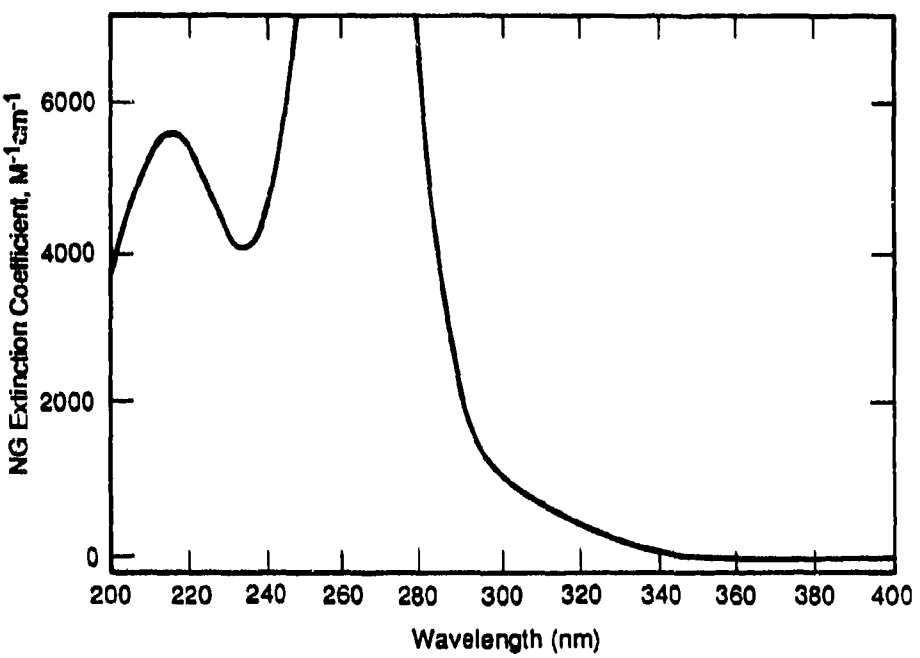


FIGURE 1 ABSORBANCE SPECTRUM OF 360 μM NG IN WATER (1 cm-cell)

TABLE 1

Molar Absorptivity and Sunlight Absorption Rates for NG at Wavelengths > 297.5 nm

| Wavelength (nm) | $L_\lambda$ [a,b] | | $\varepsilon_\lambda$, $M^{-1}cm^{-1}$ | $\varepsilon_\lambda L_\lambda$ | |
|---|---|---|---|---|---|
| | Apr 16 Spring | Jul 21 Summer | | Spring | Summer |
| 297.5 | 1.85(-5) | 6.17(-5) | 1222 | 0.02 | 0.08 |
| 300.0 | 1.06 (-4) | 2.69(-4) | 1087 | 0.12 | 0.29 |
| 302.5 | 3.99(-4) | 8.30(-4) | 978 | 0.39 | 0.81 |
| 305.0 | 1.09(-3) | 1.95(-3) | 890 | 0.97 | 1.74 |
| 307.5 | 2.34(-3) | 3.74(-3) | 811 | 1.90 | 3.03 |
| 310.0 | 4.17(-3) | 6.17(-3) | 737 | 3.07 | 4.55 |
| 312.5 | 6.51(-3) | 9.07(-3) | 665 | 4.33 | 6.03 |
| 315.0 | 9.18(-3) | 1.22(-2) | 596 | 5.47 | 7.27 |
| 317.5 | 1.20(-2) | 1.55(-2) | 528 | 6.34 | 8.18 |
| 320.0 | 1.48(-2) | 1.87(-2) | 463 | 6.85 | 8.66 |
| 323.1 | 2.71(-2) | 3.35(-2) | 376 | 10.2 | 12.6 |
| 330.0 | 9.59(-2) | 1.16(-1) | 232 | 22.2 | 26.9 |
| 340.0 | 1.23(-1) | 1.46(-1) | 93 | 11.4 | 13.6 |
| 350.0 | 1.37(-1) | 1.62(-1) | 30 | 4.11 | 4.86 |
| 360.0 | 1.52(-1) | 1.79(-1) | 8 | 1.22 | 1.43 |
| 370.0 | 1.63(-1) | 1.91(-1) | 1.8 | 0.29 | 0.34 |
| | | | | $\Sigma$ = 79.0 $d^{-1}$ | $\Sigma$ = 100.4$d^{-1}$ |

[a] $L_\lambda$ values are for 40°N latitude and are in units of Einstein-cm $L^{-1}d^{-1}$ (Federal Register, 1985).

[b] Numbers in parentheses are powers of ten.

Plots of ln $NG/NG_o$ against in $PHAP/PNAP_o$ in distilled water, KR water, and HA appear in Figure 2. All plots follow a straight line ($r^2 = 0.99$) and indicate first-order kinetic behavior. No rate enhancement was observed in KR water or HA solution, suggesting that the photolysis is not sensitized by other light-absorbing materials. Instead, NG photolysis was slowed in HA, which contained a high concentration of organics and caused light screening.

Using Equation 1 and the data in Table 1, the quantum yield for NG was calculated to be 0.011. The first-order photolysos rate constant, $k_p$, and half-life were calculated for cloudless conditions according to Equations 2 and 3 and are summarized in Table 2. The rate constant was calculated to be 1.0 $day^{-1}$ and the half-life was 0.70 days (Table 2). Using an average quantum yeidl of 0.011 and light intensity values $L_\lambda$ for other seasons, half-lives for NG of 0.8, 0.6, 1.3, and 2.3 days were calculated for the spring, summer, fall, and winter seasons, respectively, at 40°N latitude.

Photochemical Transformation Products

The photochemical transformation studies of NG described above were concluded with the identification of transformation products produced during the photolysis. Based on the structure of NG, transformation products were predicted and analytical methods were developed to detect them in photolyzed solutions. The suspected chemicals and the methods used to analyze them appear in Table 3.

Two products expected from the phototransformation were nitrate and nitrite and they were both detected by ion-exchange chromatography in photolyzed solutions. The formation of nitrite and nitrate and the loss of NG as a function of sunlight dose are shown in Figure 3 for distilled water (DW), KR water, and HA. The data indicate that the initial rate of nitrite formation is essentially the same as the initial rate of NG loss. Also, nitrate eventually accumulates at the expense of nitrite. These results suggest that nitrite is formed in a primary step and is subsequently oxidized to nitrate as shown in Scheme 1.

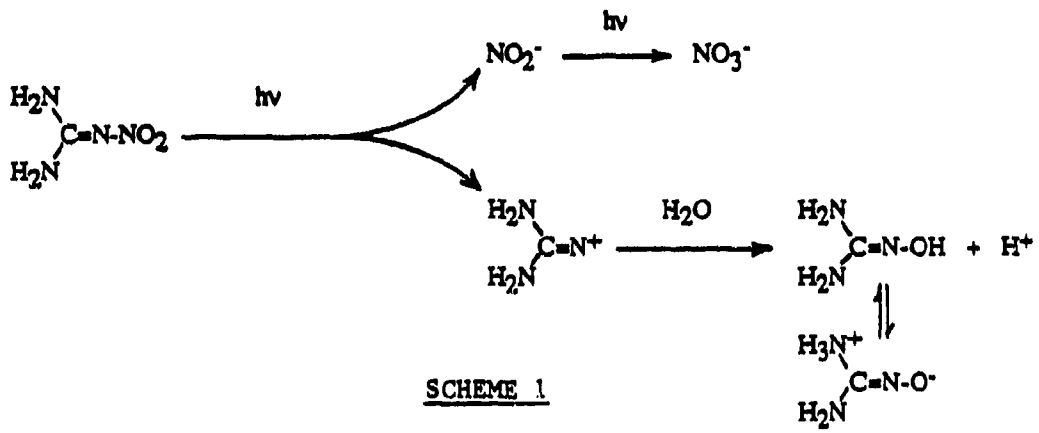


SCHEME 1

The conversion of nitrite to nitrate appears to be more rapid in KR water and HA than in DW. This finding prompted a further investigation into the photochemistry of nitrite.

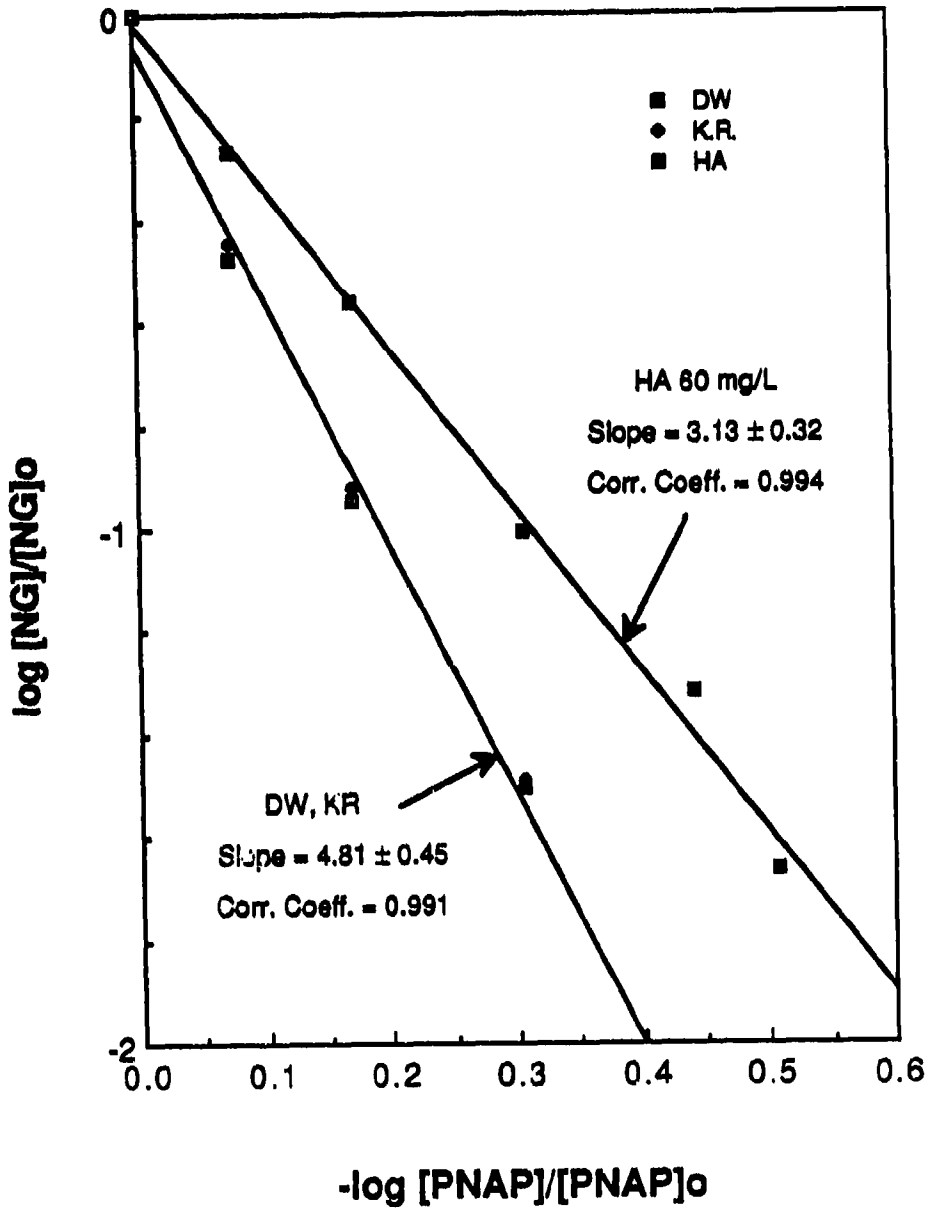


FIGURE 2 PLOTS OF $\ln NG/NG_0$ VERSUS $\ln PNAP/PNAP_0$ in sunlight in DISTILLED WATER, KANSAS RIVER WATER, AND HUMIC ACID SOLUTION. Exposure dates: May 16-22, 1986.

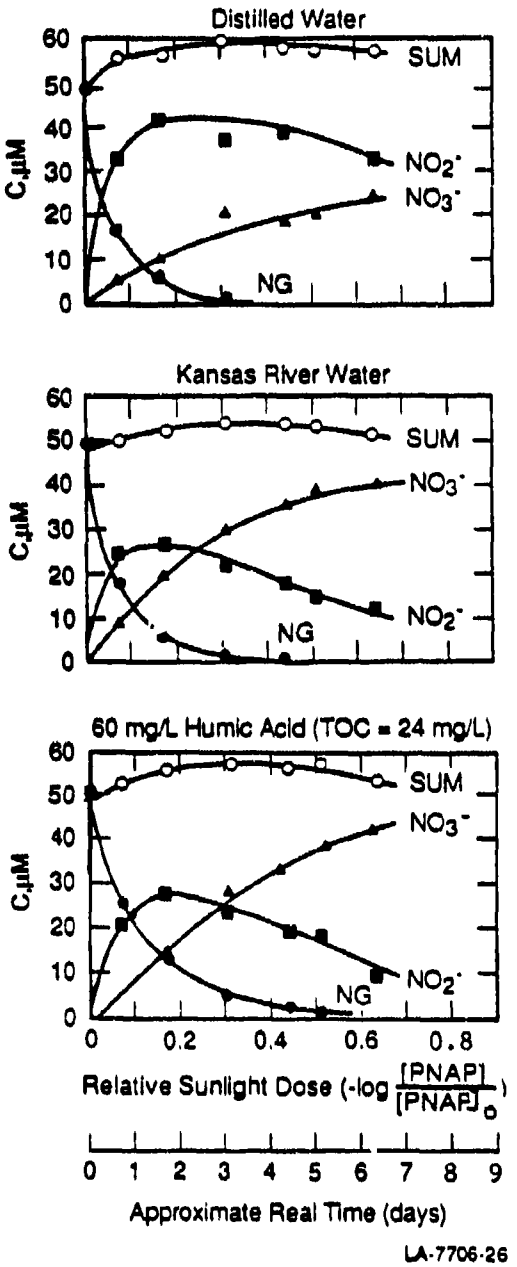


FIGURE 3 FORMATION OF NITRATE AND NITRITE AS A FUNCTION OF TIME

TABLE 2

Nitroguanidine Environmental Photolysis Quantum Yield,
Rate Constants and Half-lives[a]

| Irradiation Date (1986) | Solvent | S[b] | NG $\Sigma\epsilon_\lambda L_\lambda$, $d^{-1}$ | PNAP $\Sigma_\lambda L_\lambda$, d-1 | $\Phi_{PNAP}$ | $\Phi_{NG}$ | $k_p$, $d^{-1}$ | $t_{1/2}$, d |
|---|---|---|---|---|---|---|---|---|
| May 16-22 | DW and KR water | 4.81±0.45 | 79.0 | 430 | $4.82 \times 10^{-4}$ | 0.0126 | 1.00±0.09 | 0.70 |
| | HS[d] | 3.13±0.32 | - | - | - | - | 0.65±0.07 | 1.1 |
| July 21-24 | DW and KR water | 1.91±0.09 | 100.4 | 532 | $1.61 \times 10^{-3}$ | 0.0102 | 1.02±0.05 | 0.68 |

[a]All experiments at pH7.8, the natural pH of Kansas River Water

[b]Regression estimate slope of a plot of $\ln[NG][NG]_o$ vs $\ln[PNAP]/[PNAP]_o$±95% confidence limits of slope estimated.

[c]DW = Distilled Water with 5mM phosphate buffer. KR water had an absorbance at 313nm = 0.039$cm^{-1}$

[d]Aldrich humic solution, 60 mg/l; total organic carbon (TOC) = 24 mg/l, absorbance at 313 nm = 0.66 $cm^{-1}$

TABLE 3

Conditions for Liquid Chromatographic Analyses

| Compound | Column Type | Eluent | Retention Time, min. | Detection Mode |
|---|---|---|---|---|
| NG | C-18[a], 3 μm | $H_2O$ | 1.9 | UV, 264 nm |
| Urea | " | $H_2O$ | 1.3 | UV, 200 nm |
| NG | C-18, 10 μm | 10mM pentanesulfonic acid/1mM $H_2SO_4$ in $H_2O$ | 2.3 | UV, 190 nm |
| Guanidine | " | " | 3.6 | " |
| Hydroxyguanidine | " | " | 3.0 | " |
| Cyanamide | " | " | 2.0 | " |
| Guanidine | CS3[b] | 27.5mM HCl[c] | 4.1 | Conductivity |
| Hydroxyguanidine | " | " | 4.1 | " |
| Ammonia | " | " | 2.3 | " |
| Nitrite | AS4A[d] | 2.2mM $Na_2CO_3$/0.75mM $NaHCO_3$ | 1.9 | " |
| Nitrate | " | " | 3.9 | " |

[a]Reversed-phase, octadecylsilyl packing

[b]Dionex cation exchange column

[c]Contained 2.25mM histidine and 2.25mM 2,3-diaminopropionic acid

[d]Dionex anion exchange column

Photolysis experiments with 50 μM nitrite in aerated distilled water (Figure 4) showed that nitrite was indeed photo-oxidized to nitrate, with a half-life of about 16 days in summer and 30 days in fall. This conversion could occur by the mechanism shown in Scheme 2.

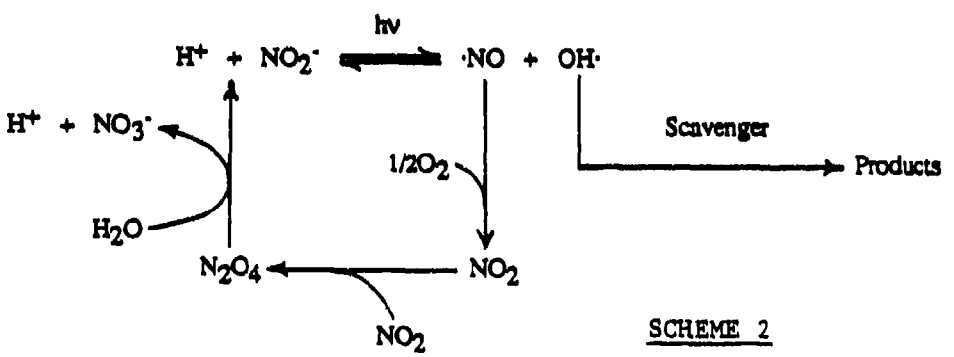


SCHEME 2

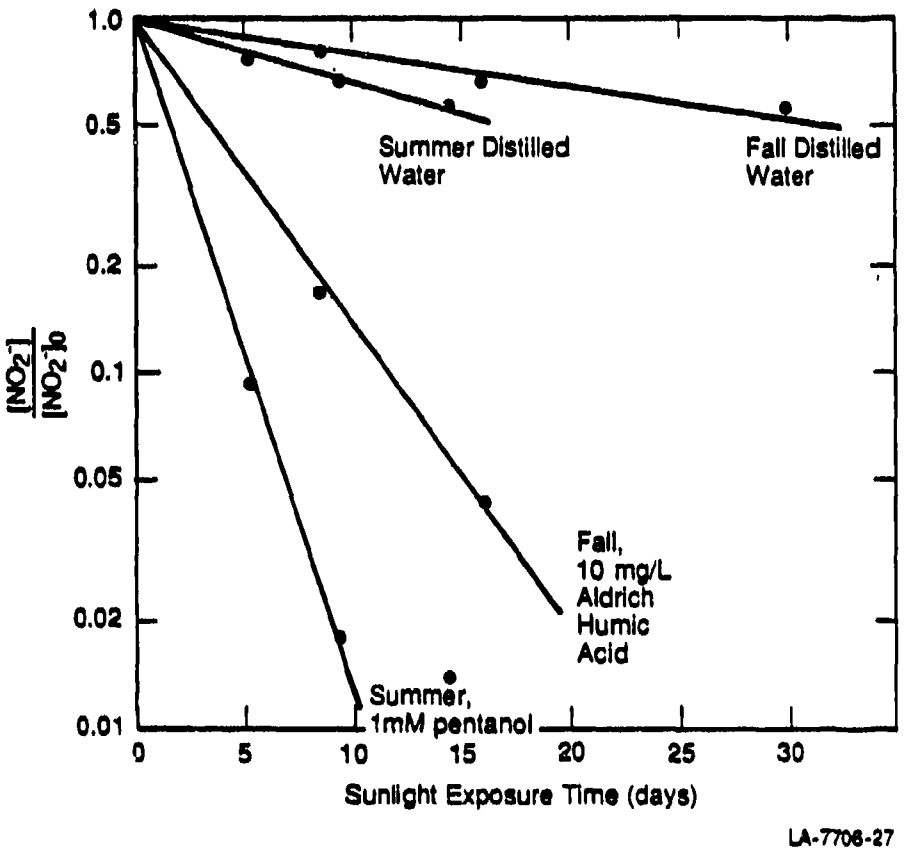


FIGURE 4 NITRITE PHOTOLYSIS IN SUNLIGHT IN QUARTZ TUBES

Figure 3 indicates nitrite is converted to nitrate more rapidly in KR and US water than in distilled water, which apparently results from the organic matter in these waters. That the presence of organic matter increases the decomposition rate of nitrite could be explained (1) by singlet oxygen or peroxy radicals whose formation is sensitized by natural dissolved organics (Zepp et al., 1977) and (2) by the scavenging of OH radicals by the organics (Mill et al., 1980). Figure 4 shows that trapping of OH radicals can be important because the addition of 1 mM pentanol, a model scavenger, dramatically increases the rate of nitrite consumption. This presumably occurs by trapping OH radicals before they can recombine with NO to regenerate nitrite (Scheme 2).

Figure 5 shows the formation of nitrate from nitrite in the absence and presence of organic matter. Humic acid and pentanol-derived radicals behave differently in that nitrite is converted completely to nitrate in HA, but 60% of the lost nitrite is unaccounted for in the presence of 1 mM pentanol.

To test the possibility that nitrite was being oxidized by singlet oxygen, we irradiated 50 μM sodium nitrite in 2 mM phosphate buffer (pH7) in the presence of 10 μM rose bengal, using the 350-watt xenon source filtered through 8 cm of a 0.05 M $NaNO_2$ solution to permit only light of $\lambda$ >400 nm. Loss of nitrite was <5% over 200 minutes, from which we calculate a second-order rate constant for reaction with singlet oxygen of less than $2 \times 10^5$ $M^{-1}s^{-1}$, using a steady state-singlet oxygen concentration of $3 \times 10^{-11}$ M as determined from the rate of furfuryl alcohol loss under the same conditions (Haag and Hoigne, 1986). Assuming an upper limit of $10^{-12}$ M singlet oxygen (Zepp et al., 1977) during our sunlight irradiations in KR water or HA, we calculate a nitrite half-life of at least 80 days in summer, which is five times slower than the observed degradation rate. So singlet oxygen cannot be important for conversion of nitrite to nitrate in natural waters.

Natural waters also produce $H_2O_2$, OH, and peroxy radicals when exposed to sunlight. Kinetic considerations indicate that direct $H_2O_2$ reaction (Edwards and Mueller, 1962) and $H_2O_2$ photolysis (Haag and Hoigne, 1985) cannot be important at typical $H_2O_2$ concentrations (<10 μM), whereas OH or peroxy radical oxidation might contribute to the rate enhancements observed.

Scheme 1 suggests that hydroxyguanidine is formed from the cation generated initially upon heterolytic cleavage of the N-N bond in NG. This compound is reported to have a pKa of about 8 and to be less stable in basic than in acid solution (Walker, 1958). It exists as a zwitterion above pH ~8 and is a strong nucleophile, resulting in potent antiviral and antitumor activity (Sapse et al., 1981). Figure 6 shows that hydroxyguanidine was formed in about 45% yield when NG was photolyzed in the xenon lamp in DW buffered at pH 8 and that it was stable to direct photolysis under these conditions. However, hydroxyguanidine formed in lower yield (14%) in KR water and its concentration began to decrease after NG had been consumed. Figure 7 shows that KR water sensitized the photolysis of hydroxyguanidine compared to distilled water. The rate constant for sensitized photolysis of hydroxyguanidine was about half the rate constant for direct photolysis of NG, and this is sufficient to explain the lower yield of hydroxyguanidine from NG in KR water.

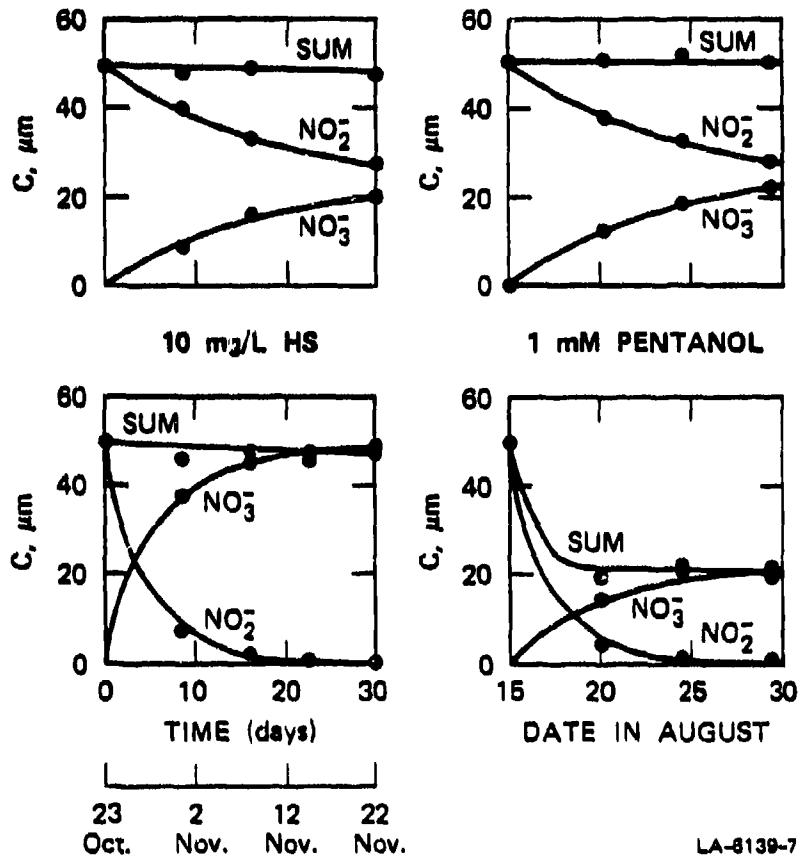


Figure 5. Formation of nitrate from nitrite during sunlight exposure in the absence and presence of organic matter.

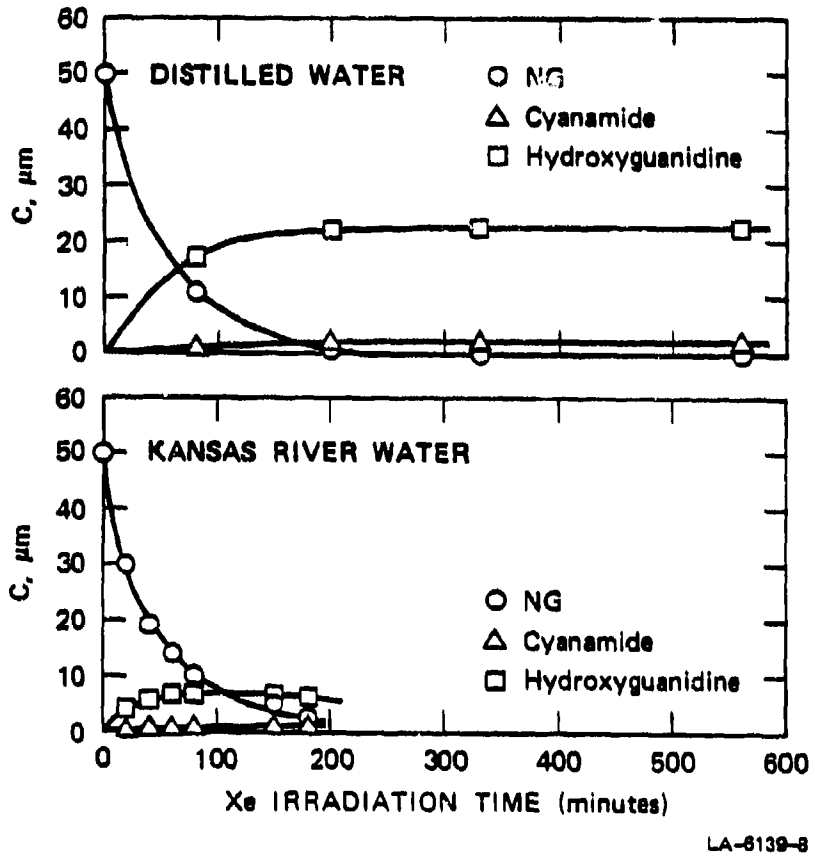


Figure 6. Photolysis products of NG in DW during irradiation in the xenon sunlamp.

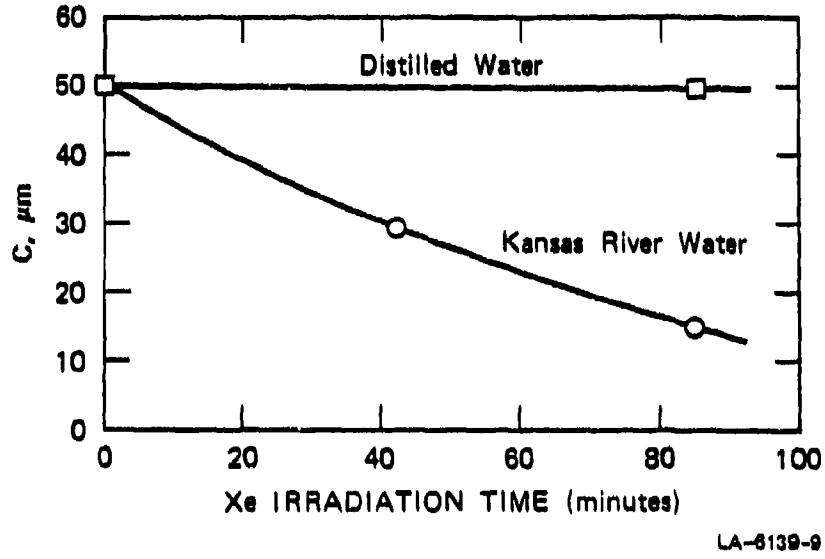


Figure 7. Photolysis of hydroxyguanidine in the xenon sunlamp in DW and KR water.

The ultimate products of NG photolysis could not be identified in the above described experiments. We found no evidence for the formation of guanidine in any experiments, even though we used chromatographic conditions in which it would have been easily detected if it had comprised as much as 10% of converted NG. Likewise, cyanamide (Figure 5), hydroxylamine, and urea (data not shown) were not formed in significant (<5%) yields, in any experiments, indicating that reactions (4) and (5) are not likely to be important.

$$H_2O + (H_2N)_2C{=}N{-}NO_2 \xrightarrow{h\nu} (H_2N)_2C{=}O + H_2N{-}NO_2 \qquad (4)$$

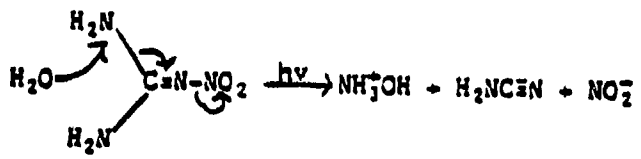

$$\xrightarrow{h\nu} NH_3^+OH + H_2NC{\equiv}N + NO_2^- \qquad (5)$$

Also, nitrite and nitrate are unlikely products of hydroxyguanidine sensitized photolysis, since only one mole of nitrite/nitrate is formed per photolyzed NG (Figure 3). Small amounts of ammonium ion were occasionally observed.

We made additional attempts to identify products by photolyzing a 1 mM NG solution for 4 days in unbuffered, distilled water, evaporating to dryness, derivatizing with bis(trimethylsilyl)trifluoracetamide (BSTFA), and analyzing by gas chromatograpy/mass spectrometry (GC/MS). The major product peaks corresponded to cyanamide ($H_2NCN$), urea, and guanidine, in order of importance.

None of these products were found in the earlier experiments with solutions containing low initial concentrations (50 µM) of substrate and containing natural or added buffers that maintained the pH near 7.8. During photolysis of 1mM NG in unbuffered water, the pH dropped from about 7 to about 3 and must have dropped further in the concentration step. The drop in pH may have altered the photolytic pathways or the stability of the products. For example, cyanamide could have formed by an acid-catalyzed breakdown of guanidine or hydroxyguanidine. Ion chromatography (IC) analysis of this solution before concentration gave a major product peak corresponding to guanidine or hydroxyguanidine and about a 10% yield of ammonium ion. A 1 mM solution of NG in KR water that was photolyzed for 5 days showed a lower yield of the guanidine/hydroxyguanidine (unresolved) peak. This may be expected because of the lower stability of hydroxyguanidine in KR water as described above. Thus, hydroxyguanidine appears to be formed during photolysis (at least transitory) in all cases.

The present photolysis kinetic results for NG agree with those obtained in our earlier screening studies and with the work of Dennis (1982). The half-life of 0.7d or 17h measured in summer is the same as that (20h) reported by Dennis (1982) for summer and about 3 times lower (50h) than we obtained in late winter in Phase I. At 40°N, sunlight intensity below 400 nm where NG absorbs is about 3 times lower in winter than in summer (Federal Register, 1985). The half-life was increased (26h) in the presence of humic acids in this study, whereas it was unaffected in the earlier study, because in the present work higher concentrations of HA were used which caused light screening.

The average quantum yield of 0.0114 is about twice that found earlier (0.0053). This is partly due to a more detailed calculation involving smaller wavelength intervals performed here, but mostly because the value of $\Sigma\varepsilon_\lambda L_\lambda$ for PNAP was too low by nearly a factor of two in the earlier study. The present values of $\Sigma\varepsilon_\lambda L_\lambda$ for PNAP results from a more precise measurement of the extinction coefficients of PNAP and updated values of $L_\lambda$, and these are the ones now given in the Federal Register (1985). In addition, the extinction coefficients for NG were remeasured, and the newer, more precise values were slightly different.

Phase I product studies showed that photolysis of NG does not yield nitrosoguanidine. A single product peak was detected by reverse-phase HPLC, which we now attribute to nitrite and/or nitrate, since it eluted with the solvent front (and therefore was very polar) and had a UV spectrum consistent with either of these ions.

## Conclusions

NG will photolyze in the environment in aqueous systems, with a surface half-life ranging from 0.6 days in summer to 2.3 days in the winter. The photolysis proceeds via a direct photolytic mechanism by which light is absorbed and the excited state NG proceeds to products with a quantum efficiency of 1%. The photolysis is not sensitized by naturally occurring humic substances. In fact, humic substances may decrease NG photolysis rates because of a screening effect (Figure 2) in which highly absorbing systems effectively compete for photons, decreasing their availability to NG. The samplings of the Kansas River that we obtained in the vicinity of the SAAP suggest that this aqueous system is very transparent and that photolyses in the top 20 cm should proceed at the rates measured.

The photochemical transformation initially yields nitrite and hydroxyguanidine. Nitrite is photochemically transformed to nitrate. Hydroxyguanidine undergoes sensitized photolysis in Kansas Riverwater at a rate about half as high as nitroguanidine direct photolysis, and leads to unidentified products.

## TASK 2

### Photochemical Transformation of Diethyleneglycol Dinitrate and Identification of Photochemical Transformation Products

#### Introduction

Diethyleneglycol dinitrate (DEGDN) is a nitrate ester produced and used by the military as a propellant compound. It is manufactured at the Radford Army Ammunition Plant (RAAP) located in Radford, Virginia. Wastewaters containing DEGDN and produced at RAAP are transported by underground pipelines to a biological treatment facility prior to discharge to the New River.

The objectives of this task were to determine the first-order photolysis rate constant, $k_p$, the quantum yield, $\Phi_c$, and photochemical transformation products of DEGDN. The quantum yield was determined by monitoring the loss of DEGDN as a function of sunlight dose, which is measured by an aqueous p-nitroacetophenome/pyridine (PNAP/PYR) actinometer solution. Details of the rate methodology have been described by Dulin and Mill (1982). A plot of ln[DEGDN] versus the ln[PNAP] yields a straight line of slope S, from which $\Phi_c$ can be calculated using Equation 6.

$$\Phi_c = \Phi_{PNAP} \frac{S\Sigma\varepsilon_\lambda^{PNAP} L_\lambda}{\Sigma\varepsilon_\lambda^{c} L_\lambda} , \qquad (6)$$

where

$\Phi_{PNAP}$ = quantum yield for the actinometer

$\varepsilon_\lambda^{PNAP}$ = molar absorptivity of PNAP at wavelength $\lambda$

$\varepsilon_\lambda^{c}$ = molar absorptivity of DEGDN at wavelength $\lambda$

$L_\lambda$ = sunlight intensity at wavelength $\lambda$ for a given time of year

From $\Phi_c$ the first-order photolysis rate constant, $k_p$, can be calculated according to Equation 7 and the half-life, $t_{1/2}$, by Equation 8.

$$k_p = \Phi_c \Sigma\varepsilon_\lambda^{c} L_\lambda = S\Phi_{PNAP}\Sigma\varepsilon_\lambda^{PNAP} L_\lambda \qquad (7)$$

$$t_{1/2} = 0.69/k_p \qquad (8)$$

From equations 6, 7, and 8 it is possible to project the persistence of DEGDN in aqueous systems as a function of the water body and sunlight intensity (season).

## Materials and Methods

DEGDN was obtained from Hercules, Inc. as a yellow liquid containing 15% acetone (Lot No. RAD 821M005214). The acetone was rotary-evaporated at room temperature to produce a yellow oil. The oil was dissolved in distilled water or 60 mg/l HA, both buffered at pH7.8 with 5mM phosphate, or in unbuffered KR water, to produce concentrations of 61 μM for photolytic studies.

Irradiations were performed in sunlight from 24 June to 8 August 1986 in quartz tubes (1 cm o.d.) held on a rack at 30° from the horizon. The sunlight flux was monitored using p-nitroacetophenone/pyridine (PNAP/PYR) actinometers (Dulin and Mill, 1982). At each time point, actinometer and sample tubes were removed and stored in the dark at 3°C until analysis at the end of the run. A single tube was collected per time point for each matrix, approximately once every 6 days.

DEGDN was monitored by high-performance liquid chromatography (HPLC) using an HP1090 liquid chromatograph, a 6-cm, 3 μm $C_{18}$ reverse-phase column, 1:1 acetonitrile:water eluent at 0.4 mL/min, and UV detection at 200 nm. The conditions used for DEGDN and suspected transformation products appear in Table 4.

TABLE 4

Conditions for Liquid Chromatographic Analysis--DEGDN

| Compound | Column Type | Eluent | Retention Time, min. | Detector |
|---|---|---|---|---|
| PNAP | C-18 | 1:1 $H_2O$:MeCN | 3.3 | UV, 275 nm |
| DEGDN | " | " | 4.6 | UV, 200 nm |
| Formic acid | " | 5mM $Na_2B_4O_7$ | 2.0 | Conductivity |
| Acetic acid | " | " | 1.7 | " |
| Glycolic acid | " | " | 1.7 | " |
| Glyoxylic acid | " | " | 2.0 | " |
| Nitrite | " | 2.2mM $Na_2CO_3$\|0.75mM $NaHCO_3$[a] | 2.2 | " |
| Nitrate | " | " | 4.3 | " |

[a]With NG1 guard column.

Additional product studies were performed by exposing a 1mM solution of DEGDN in unbuffered, distilled water in a 50-mL in quartz tubes to sunlight from 24 June to 8 August 1986. A second set of tubes were exposed from 20 August to 8 October 1986. HPLC analysis of the latter solutions showed 14% DEGDN remaining at the end of the reaction. Dark controls were kept at room temperature. The first photolyzed solution was evaporated to dryness, derivatized with BSTFA, and analyzed on a Ribermag R10-10C GC/MS system using a 15-m DB-5 column and electron impact ionization at 70 eV. The second solution was analyzed by ion chromatography and an aliquot was derivatized with phenyldiazomethane according to the procedure of Ovenberger and Anselme (1963). The derivatized solution was concentrated and subject fo GC/MS analysis on an HP5980 gas chromatograph equipped with a J&W 1701 column and an HP5970 mass selective detector.

Absorption spectra were obtained on an HP 8450A spectrophotometer. A 10mM DEGDN solution was prepared in 3:1 water:acetonitrile and measured in a 10-cm cell. A 1.0 DEGDN solution was prepared in 19:1 ethanol:water and measured in a 1-cm cell. Extinction coefficients below 320 nm were averaged.

## Results

### Photolysis Results

The ultraviolet absorption spectrum of DEGDN appears in Figure 8. Because it is not possible to accurately measure the spectrum in pure water due to solubility limitations, we used 25%/75% acetonitrile/water and 95%/5% ethanol/water as solvents. The extinction coefficients below 320 nm in the two solvent systems agreed within 10%, indicating no large effect of solvent. The measured values should therefore closely approximate those in pure water. The molar absorptivity ($\epsilon_\lambda$) at various wavelengths above 297.5 nm, the light intensity for spring and summer months ($L_\lambda$), and the product of $\epsilon_\lambda L_\lambda$ for spring and summer are listed in Table 5.

Plots of the ratio of $\ln[DEGDN]/[DEGDN]_o$ versus $\ln[PNAP]/[PNAP]_o$ for distilled water (DW) and Kansas River (KR) water gave nearly identical loss curves, (Figure 9). Based on the results with NG, HA was expected to cause light screening and slow the photolysis of DEGDN. The fact that no rate reduction, but possibly even a slight rate increase occurred, suggests that some sensitization compensates for light screening. The rate constants and quantum yields for each solution appear in Table 6. From these data, half-lives of 19, 15, 33, and 59 days were calculated for the spring, summer, fall, and winter seasons, respectively, at 40°N latitude. These half-lives are affected only slightly by high concentrations of humic substances and not at all by the natural solutes present in the KR water.

### Photochemical Transformation Products

The photochemical transformation studies of DEGDN described in Task 2 were concluded with the identification of transformation products.

The initial studies followed the formation of nitrite and nitrate by ion chromatography as a function of DEGDN concentration loss. Plots of the loss of DEGDN and nitrite and nitrate formation appear in Figure 10 for DW water, and HA. Figure 10 indicates that nitrate is the major inorganic product of

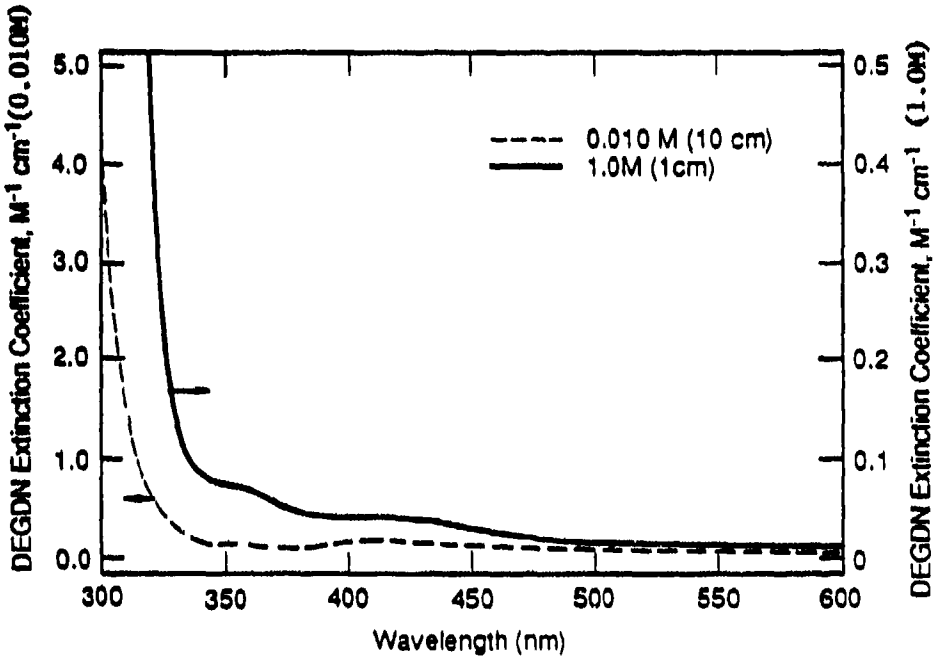


FIGURE 8. ABSORPTION SPECTRUM OF DEGDN IN 25%/75% ACETONITRILE/WATER (0.010M) AND IN 95% ETHANOL/5% WATER (1.0M)

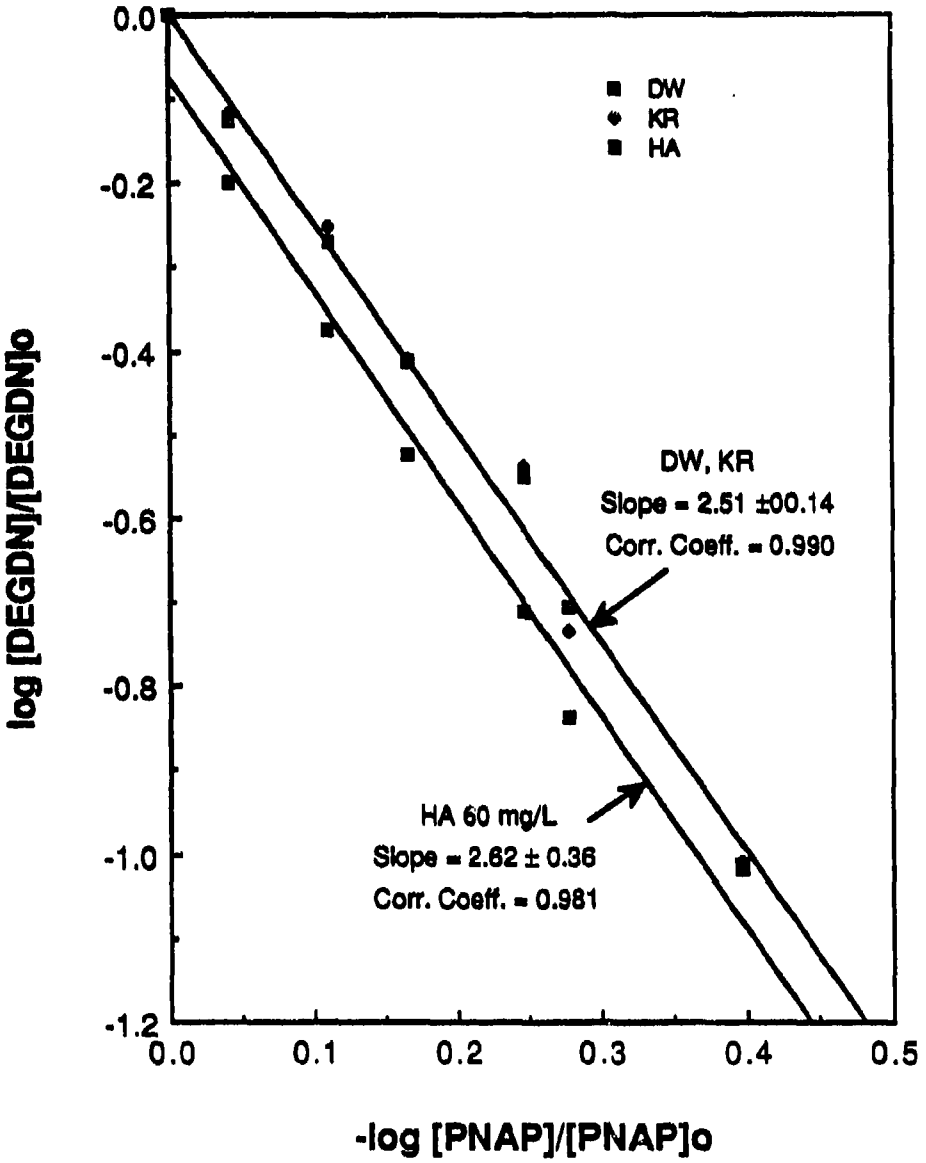


FIGURE 9. PLOTS OF ln [DEGDN]/[DEGDN]$_0$ VERSUS ln [PNAP]/[PNAP]$_0$ IN SUNLIGHT IN DISTILLED WATER, KANSAS RIVER WATER, AND HUMIC ACID SOLUTION

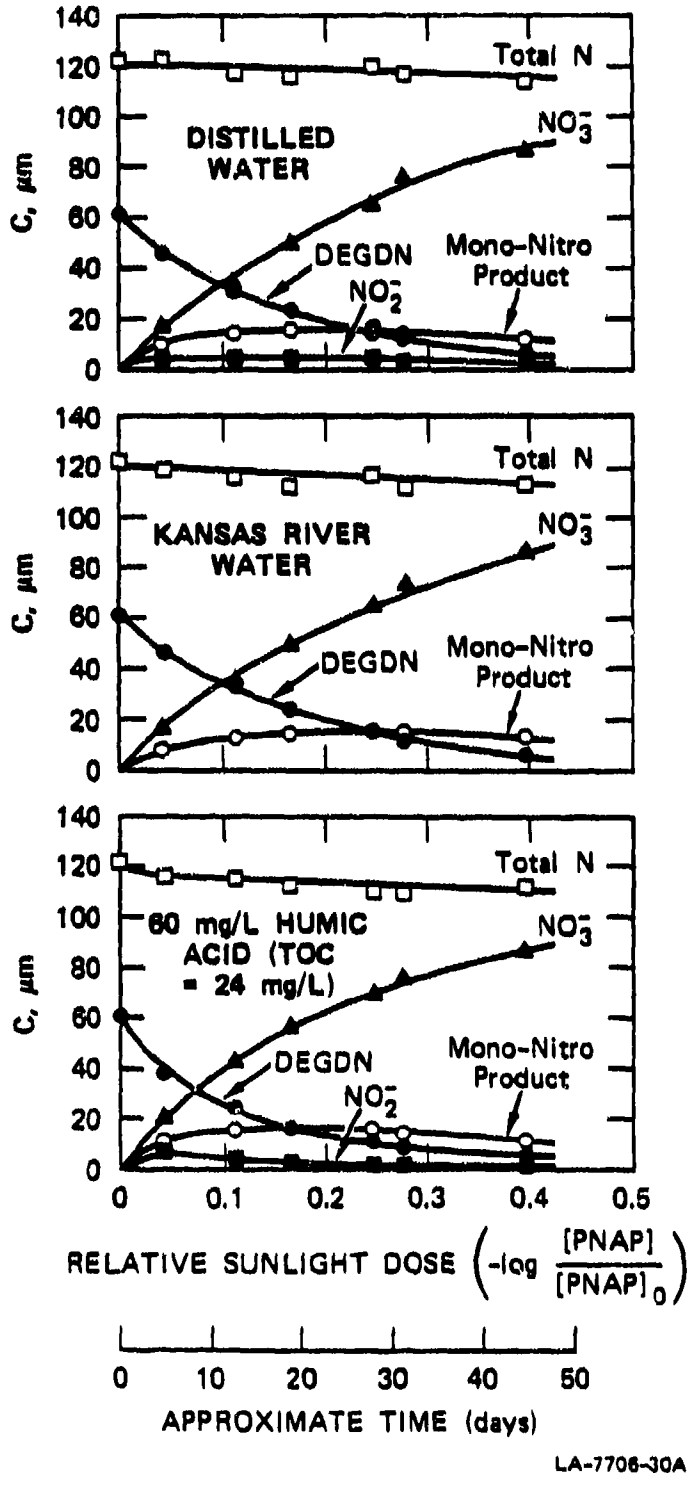


Figure 10. Product formation during photolysis of DEGDN.

TABLE 5

Calculation of Sunlight Absorption Rates for DEGDN

| λ nm | $L_\lambda$ at 40°N Latitude[a,b] April 16 Spring | Jul 21 Summer | Spring DEGDN ($\varepsilon_\lambda$, $M^{-1}$ $cm^{-1}$) | Summer DEGDN ($\varepsilon_\lambda L_\lambda$) |
|---|---|---|---|---|
| 297.5 | 1.85 (-5) | 6.17 (-5) | 5.9 | 0.00036 |
| 300.0 | 1.06 (-4) | 2.69 (-4) | 4.6 | 0.00124 |
| 302.5 | 3.99 (-4) | 8.30 (-4) | 3.5 | 0.0029 |
| 305.0 | 1.09 (-3) | 1.95 (-3) | 2.8 | 0.0055 |
| 307.5 | 2.34 (-3) | 3.74 (-3) | 2.1 | 0.0079 |
| 310.0 | 4.17 (-3) | 6.17 (-3) | 1.7 | 0.0105 |
| 312.5 | 6.51 (-3) | 9.07 (-3) | 1.3 | 0.012 |
| 315.0 | 9.18 (-3) | 1.22 (-2) | 0.94 | 0.0115 |
| 317.5 | 1.20 (-2) | 1.55 (-2) | 0.70 | 0.0109 |
| 320.0 | 1.48 (-2) | 1.87 (-2) | 0.50 | 0.0094 |
| 323.1 | 2.71 (-2) | 3.35 (-2) | 0.29 | 0.0097 |
| 330.0 | 9.59 (-2) | 1.16 (-1) | 0.13 | 0.015 |
| 340.0 | 1.23 (-1) | 1.46 (-1) | 0.073 | 0.0107 |
| 350.0 | 1.37 (-1) | 1.62 (-1) | 0.064 | 0.0104 |
| 360.0 | 1.52 (-1) | 1.79 (-1) | 0.057 | 0.0102 |
| 370.0 | 1.63 (-1) | 1.91 (-1) | 0.046 | 0.0088 |
| 380.0 | 1.74 (-1) | 2.04 (-1) | 0.037 | 0.0075 |
| 390.0 | 1.64 (-1) | 1.93 (-1) | 0.034 | 0.0066 |
| 400.0 | 2.36 (-1) | 2.76 (-1) | 0.032 | 0.0088 |
| 410.0 | 3.10 (-1) | 3.64 (-1) | 0.032 | 0.0116 |
| 420.0 | 3.19 (-1) | 3.74 (-1) | 0.031 | 0.0116 |
| 430.0 | 3.08 (-1) | 3.61 (-1) | 0.029 | 0.0105 |
| 440.0 | 3.65 (-1) | 4.26 (-1) | 0.025 | 0.0107 |
| 450.0 | 4.11 (-1) | 4.80 (-1) | 0.021 | 0.0101 |
| 460.0 | 4.16 (-1) | 4.85 (-1) | 0.017 | 0.0082 |
| 470.0 | 4.30 (-1) | 5.02 (-1) | 0.013 | 0.0065 |
| 480.0 | 4.40 (-1) | 3.14 (-1) | 0.010 | 0.0051 |
| 490.0 | 4.16 (-1) | 4.86 (-1) | 0.0072 | 0.0035 |
| 500.0 | 4.25 (-1) | 4.96 (-1) | 0.0054 | 0.0027 |
| 525.0 | 1.12 1.31 | 0.0027 | 0.0035 | |
| 550.0 | 1.16 1.36 | 0.0016 | 0.0022 | |
| 575.0 | 1.17 1.37 | 0.0007 | 0.0010 | |
| 600.0 | 1.18 1.38 | 0.0004 | 0.0006 | |
| 625.0 | 1.20 1.40 | 0.0002 | 0.0003 | |
| 650.0 | 1.21 1.41 | 0.0001 | 0.0001 | |
| | | | $0.248 d^{-1}$ | |
| 675.0 | 1.22 1.41 | | | |
| 700.0 | 1.21 1.40 | | | |
| 750.0 | 2.33 2.69 | | | |
| 800.0 | 2.25 2.59 | | | |

[a] $L_\lambda$ in units of milliEinsteins $L^{-1}d^{-1}$.
[b] Numbers in parentheses are powers of ten.

TABLE 6

Diethyleneglycol Dinitrate Environmental Quantum Yield, Photolysis Rate Constants, and Half-life[a]

| Irradiation Date (1986) | Sample Matrix | S[b] | $\Sigma\epsilon_\lambda DEGDN_{L_\lambda}, d^{-1}$ | $\Sigma_\lambda^{PNAP} L_\lambda, d^{-1}$ | $\phi_{PNAP}$ | $\phi_{DEGDN}$ | kp, $d^{-1}$ | $t_{1/2}$, d |
|---|---|---|---|---|---|---|---|---|
| June 24-Aug. 8 1986 | DW and Kansas River Water[c] | 2.51±0.14 | 0.248 | 532 | $3.38 \times 10^{-5}$ | 0.182 | 0.045±0.003 | 16 |
| | Humic Acid Solution[d] | 2.62±0.36 | - | - | - | - | 0.047±0.006 | 15 |

[a]All experiments performed at pH7.8, the natural pH of Kansas River Water

[b]Regression estimate slope of a plot of ln [DEGDN]/$[DEGDN]_o$ vs. ln[PNAP]/$[PNAP]_o$ ± 95% confidence limits.

[c]DW = Distilled Water with 5mM phosphate buffer. KR water had an absorbance at 313 = 0.039$cm^{-1}$

[d]Aldrich humic solution, 60 mph; TOC = 24 mg/l, absorbance at 313 nm = 0.66 $cm^{-1}$

DEGDN photolysis and that its rate of formation is not significantly different in DW, KR water, or HA. Nitrite is formed in a low, steady-state concentration. Nitrite in KR water could not be measured accurately by ion chromatography at these low concentrations because of interference by a large chloride peak.

The following kinetic analysis shows that nitrite is not a dominant precursor in the formation of nitrate. From the above described (Figure 5) studies on the photolysis of nitrite, we determined a rate constant $k_p$ of 0.043 $d^{-1}$ for the photochemical conversion of nitrite to nitrate in distilled water. Using a steady state concentration of 4 μM nitrite (Figure 10), the calculated rate of nitrate formation is:

$$+d[NO_3^-]/dt = k_p[NO_2^-] = 0.043d^{-1}(4\ \mu M) = 0.17\ \mu M{\cdot}d^{-1}$$

This is an order of magnitude lower than the observed nitrate formation rate of 2-3 $\mu M{\cdot}d^{-1}$ over the first 30 days in distilled water (Figure 10). Thus, it appears that nitrate is formed directly in the photolysis of DEGDN.

For the experiments illustrated in Figure 10, reverse-phase HPLC analysis with diode array detection showed the formation of a product which was more polar (had shorter retention time) than DEGDN but had an identical UV spectrum (Figure 11). (Although the data in Figure 11 are for 1mM DEGDN in unbuffered water, similar results were obtained in the kinetic studies described in Figure 10). These results suggest that a polar organic compound, possibly an alcohol, was being formed which still contained one nitro group.

When the aqueous, photolyzed DEGDN solution was evaporated to near dryness and derivatized with BSTFA, one major detectable product was observed that yielded a molecular weight of 237 by gas chromatography/mass spectrometry and a mass spectrum (Figures 12a and 12b) consistent with 2-hydroxethyl-nitratoacetate (I) as the trimethylsilyl ether.

(I)

This structure is also consistent with the product found by HPLC at lower concentration of DEGDN (experiments in Figure 10). To quantitate the amount of mono-nitro product, we assumed that its extinction coefficient is one-half as large as that for DEGDN, a reasonable assumption since the absorbance above 200 nm for both compounds should be dominated by the nitrato chromophore and because absorbance by isolated chromophores should be additive. From the peak heights of the mono-nitro product reltive to that of DEGDN at time zero we estimated the concentrations of the product shown in Figure 10. This allowed us to calculate the total nitrogen recovered; a mass balance is achieved within 10% in all waters.

The mono-nitro product (compound I) clearly photolyzes further, since nitrate is formed in concentrations greater than the original DEGDN concentration. The products of further photolysis are expected to be nitrate and polar, non-UV-absorbing organic compounds, which are difficult to analyze. Ion chromatography of a photolyzed 1mM DEGDN solution in DW is shown in Figure 13.

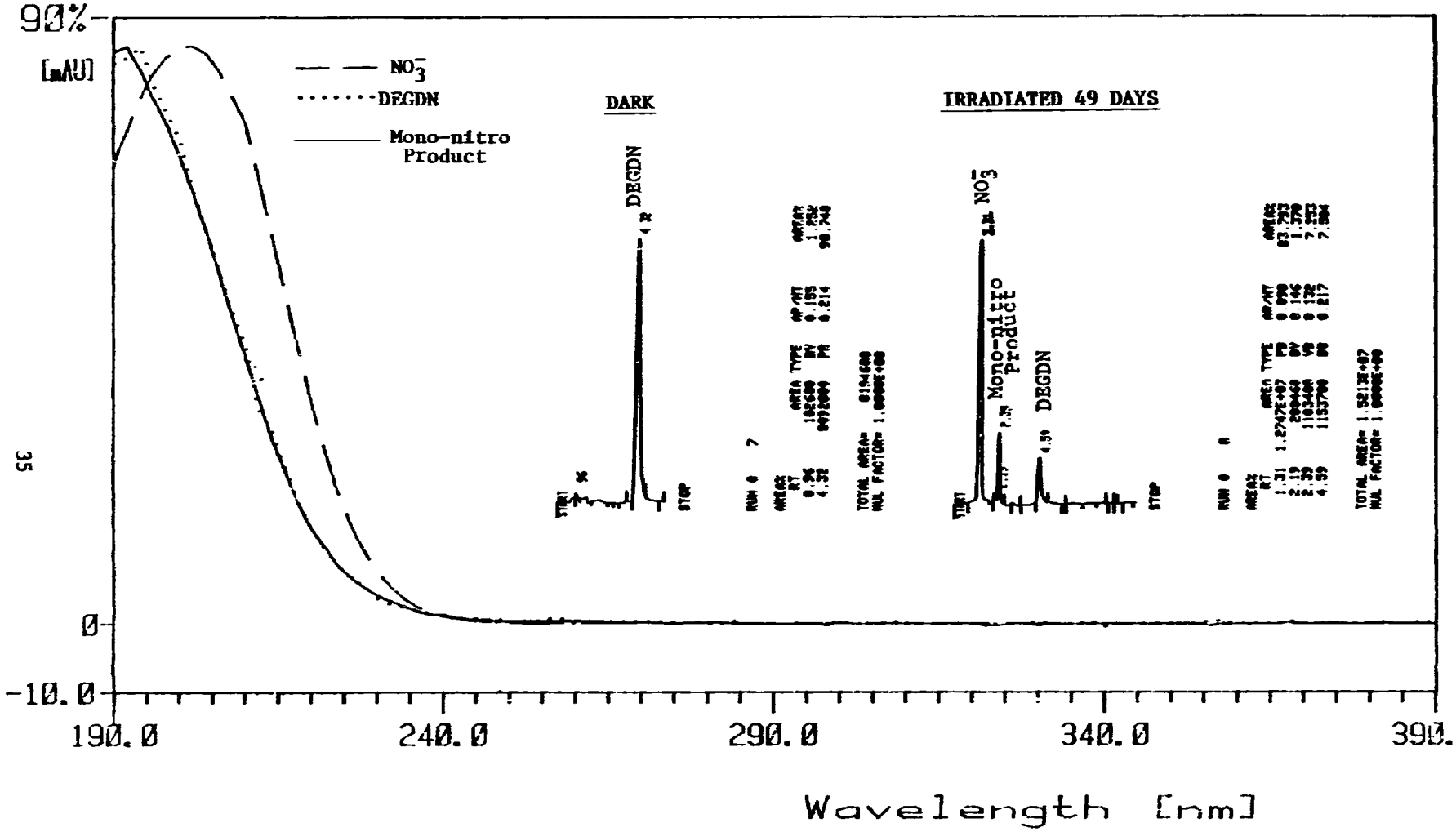


FIGURE 11. UV SPECTRA OF PRODUCTS DETERMINED BY HPLC OF 1 mM DEGDN IN THE DARK AND PHOTOLYZED FROM 20 AUGUST TO 7 OCTOBER 1986.

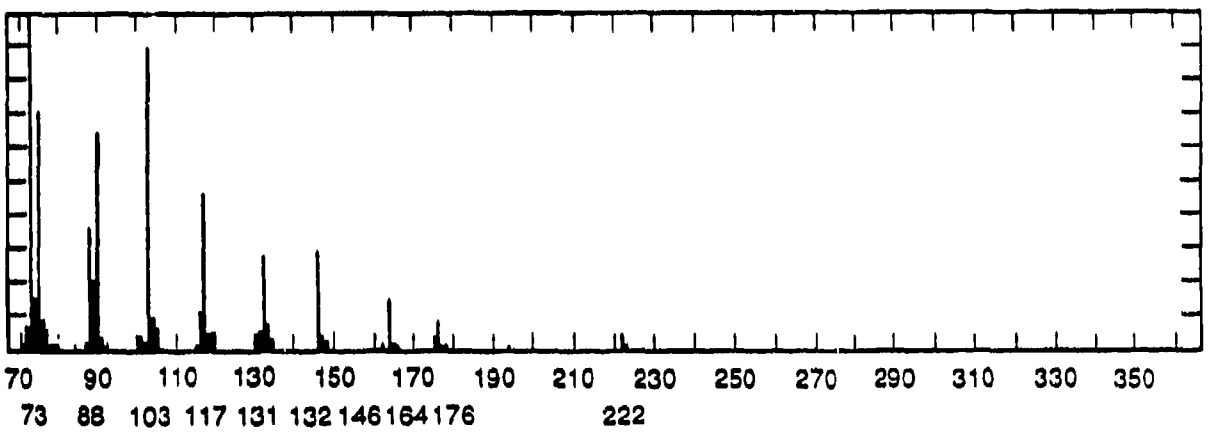


Figure 12a DEGDN PHOTOLYSIS PRODUCT – ELECTRON IMPACT SPECTRUM

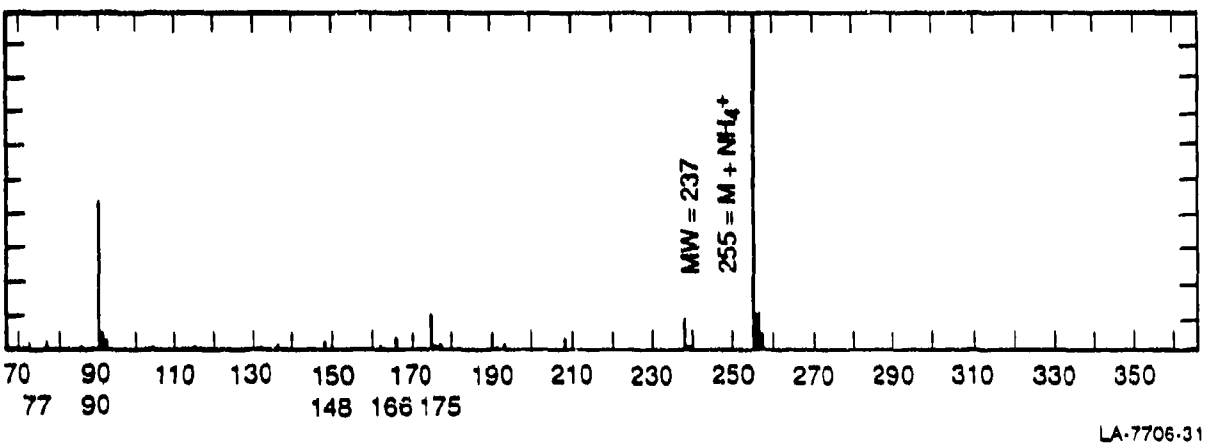


Figure 12b DEGDN PHOTOLYSIS PRODUCT-- $NH_3$ CHEMICAL IONIZATION SPECTRUM

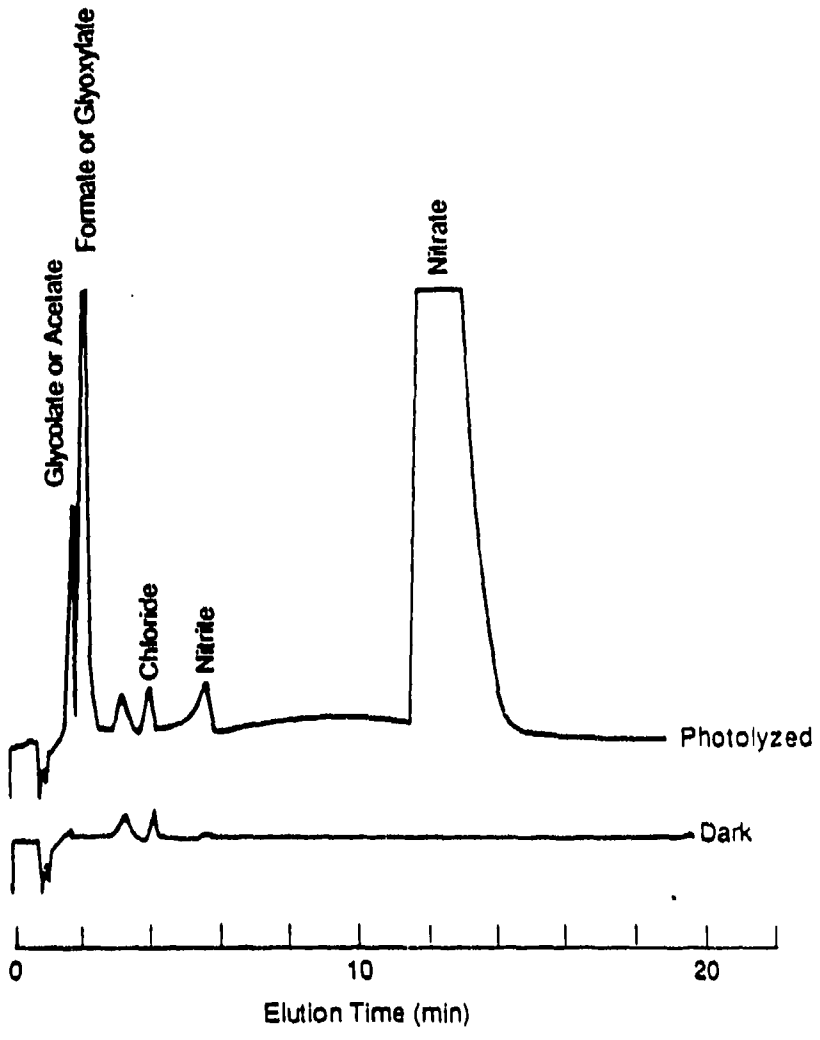


FIGURE 13. FORMATION OF ANIONIC PRODUCTS DURING THE SUNLIGHT PHOTOLYSIS OF 1mM DEDGN IN DISTILLED WATER

Figure 13 showed the formation of small organic acids in distilled water. We suspected these acids to be glycolic acid and formic acid; however, we could not resolve them from acetic acid and glyoxylic acid, respectively. Acetic acid formation is extremely unlikely since it would require reduction of one of the C-O bonds and therefore we attribute the first peak to glycolic acid.

Verification that formic acid is produced was obtained by GC/MS analysis of a phenyldiazomethane-derivatized aliquot of a photolyzed solution of 1mM DEGDN in DW (Overberger and Anselme, 1963). Such analysis yielded the benzyl ester of formic acid as the only identifiable acidic product. Assuming then that the formate/glyoxylate peak in Figure 3 is all due to formate, the yield of formate was 74% of the starting DEGDN based on aqueous standards of potassium formate. Similarly, the yield of acetate/glyoxylate was about 4% for either of these two acids.

A plausible scheme for the aqueous photolysis of DEGDN is shown in Scheme 4.

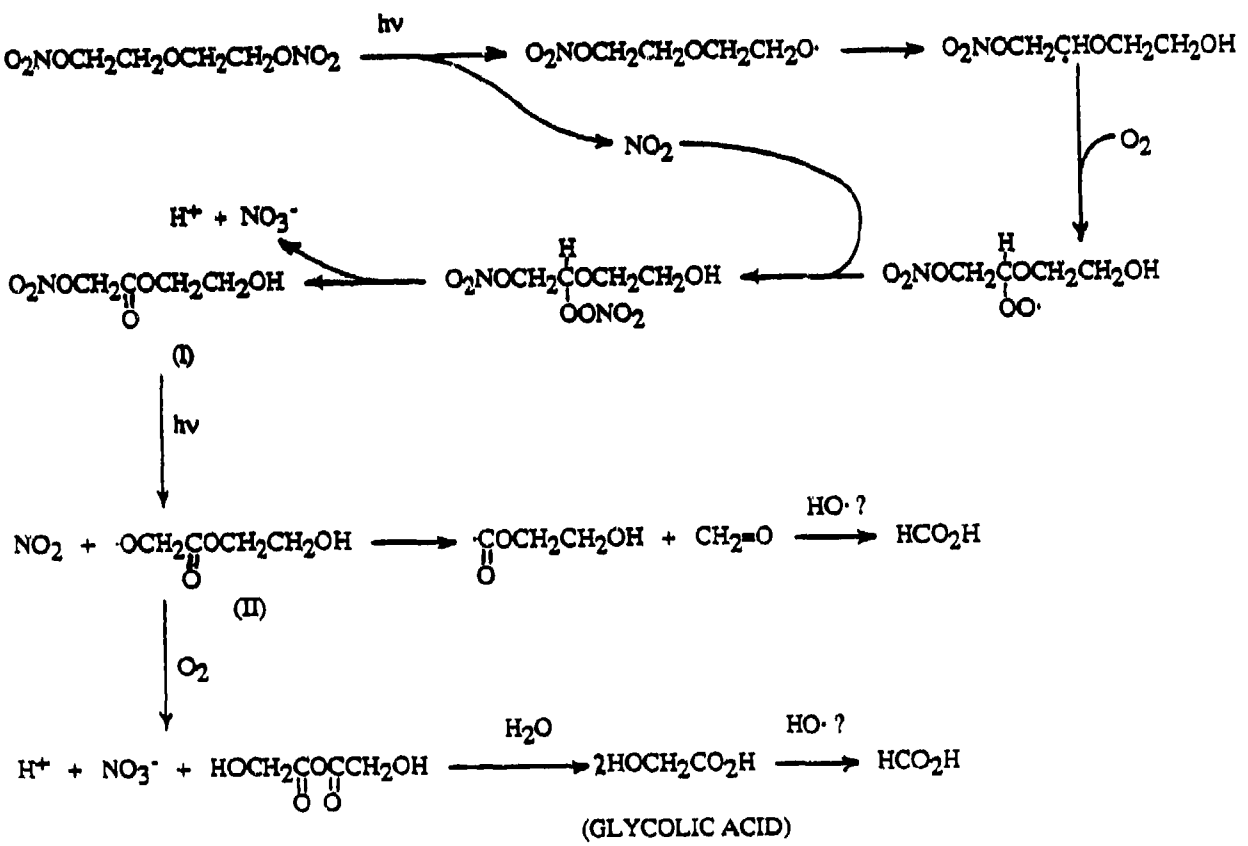


SCHEME 4

Alkyl nitrates are known to photolyze at the RO-N bond, yielding $NO_2$ and an alkoxy radical (Barltrop and Coyle, 1975). $NO_2$ forms nitrite and nitrate by disproportionation as in Scheme 2. The alkoxy radical undergoes further decomposition by an internal hydrogen abstraction and oxidation.

If compound (I) photolyzes by a mechanism analogous to that for DEGDN, the anhydride of glycolic acid would be produced, and this anhydride would hydrolyze to glycolic acid in water. Formic acid may arise from oxidation of glycolic acid or from radical (II), which can break down to form formaldehyde, which is subsequently oxidized. It is known that solutions of nitrite and nitrate photolyze to give low concentrations of hydroxyl radicals which can oxidize organics to small acids (Haag and Hoigne, 1985). Such oxidation would be inhibited by natural organics which compete for $OH_+$ radicals. Thus, the ultimate products may depend on the scavenging ability of the water and the amount of nitrate formed (initial concentration of DEGDN).

Phase I photolysis studies on DEGDN gave an estimated environmental quantum yield of 0.037, which is a factor of 5 lower than found in Phase II ($\Phi$=0.18). There are several reasons for this difference, the most important of which is that the previous work used a value of $\Sigma\varepsilon_\lambda L_\lambda$ for PNAP which was low by a factor of about 3, as described above for NG. Less important differences are that the earlier work 1) used borosilicate vials instead of quartz tubes, the former of which could have filtered out a small fraction of the sunlight below 320 nm, 2) used Spring $L_\lambda$ values in the calculations but irradiations were performed in early summer, 3) used $\varepsilon_\lambda$ values for DEGDN determined at lower concentration, which were inherently less accurate for the weak absorbance tail extending to wavelengths up to nearly 650 nm, 4) used an actinometer which photolyzed about 30 times faster than DEGDN, making correlation of the two rates less accurate.

## Conclusions

DEGDN has little absorption in the solar spectral region and a low light-absorption rate ($\varepsilon_\lambda L_\lambda$ = 0.248 $d^{-1}$). However, the light that is absorbed allows DEGDN to photolyze at an efficiency of 18% ($\Phi_c$ = 0.182). From the first-order photolysis rate constant, half-lives ranging from 15 days in the summer to 59 days in the winter were determined. A slight rate-enhancing effect was observed in highly absorptive waters (A = 0.66); however, this effect is expected to be negligible in most natural water environments.

The results of this study suggest 2-hydroxyethylnitratoacetate, nitrate, glycolic acid, and formic acid as the major photochemical transformation products of DEGDN. Nitrogen balance indicates that all N is ultimately converted to nitrate. The incomplete carbon balance indicates that polar, non-UV-absorbing carbon compounds must also be formed to some extent, but these could not be identified.

## TASK 3

### Biotransformation of Hexachloroethane and Identification of Biotransformation Products

#### Introduction

Hexachloroethane (HCE) is the major organic component of HCE screening smoke used by the military to screen equipment and personnel. In Phase I (Spanggord et al., 1985), we found that microorganisms from local natural waters could transform HCE. The biotransformation occurred by a cometabolic process and the microorganisms apparently could not utilize HCE as a sole carbon and energy source. The objective of this task was to determine the rate constant for the HCE biotransformation and to identify biotransformation products.

The biotransformation rate study was conducted with a large microbial population grown in a complex organic nutrient medium containing yeast extract. Under these conditions, the biotransformation proceeds by a pseudo-first-order rate process with respect to HCE as shown in Equation 9.

$$\frac{dC}{dt} = k_b^1[C] \qquad \text{Eq. (9)}$$

where $k_b^1$ is the pseudo-first-order rate constant and C is the HCE concentration. Integration of Equation 9 yields Equation 10.

$$\ln C_o/C_t = k_b^1, \qquad \text{Eq. (10)}$$

where $C_o$ and $C_t$ are the concentration of chemical at time zero and at time t (time t does not include the lag-phase period). By plotting ln C as a function of time, $k_b^1$ can be determined as the slope of the line by a least-squares regression analysis. $k_b^1$ is a function of microbial population [X]. The microbial population can be determined by a plate count. Once this value is known, the second-order biotransformation rate constant can be determined by Equation 11.

$$k_{b2} = k_b^1/[X] \qquad \text{Eq. (11)}$$

Although aerobic bacteria can biotransform HCE, volatilization will predominate as the major fate pathway in an aerobic surface water. However, biotransformation will become predominant in anaerobic deep waters. The rate, therefore, was studied with the use of sealed bottles to minimize the effect of volatilization.

## Methods

Microorganisms from two locations in two local waters and ATCC organisms used in the biosorption study all possessed the ability to biotransform HCE as reported in the Phase I studies. For the kinetic studies, microorganisms were obtained from Coyote Creek water (San Jose, CA) and grown in 1 liter basal salts medium plus 1 $g^{-1}$ yeast extract with 10ppm of HCE (added from a 50mg/ml DMSO stock solution and incubated in a 1-liter bottle with a Teflon-lined screw cap. After several days, the organisms were transferred to identical medium containing 10 ppm HCE in a Teflon-lined, screw-capped, 1-liter bottle and mixed with a magnetic stir-bar. Periodically, 2 ml of broth was extracted with 2 ml of diethyl either containing the internal standard o-nitrotoluene, and re-extracted with 1 ml of diethyl ether. The ether extracts were combined and analyzed by gas chromatography (GC) under the following conditions.

Instrument: Hewlett-Packard 5730 gas chromatograph

Column: 1.8 m x 2 mm glass column packed with 10% DC-200 on 80/100 mesh chromosorb W-HP

Flow Rate: 37 ml/min of 5% methane in argon

Temperature: 110°C isothermal

Detector: Electron capture -$^{63}$Ni

Retention Time: 4.35 min, hexachloroethane; 6.20 min, o-nitrotoluene (internal standard).

Quantitation was achieved by the internal standard method, using o-nitrotoluene as the internal standard and a Hewlett-Packard 3380A digital integrator.

After several transfers, 90% of the HCE was usually metabolized in six or seven days.

After six days of incubation, the microorganisms were centrifuged at 4000 x G for 10 minutes, washed with 1 g/L phosphate buffer (pH 7.0), and centrifuged again. The cells were resuspended in 1/15 of the original volume of phosphate buffer. The cell suspensions (60 ml) were transferred into two 60-ml crimp-top reaction vials and the vials were sealed with Teflon-silicon disc septa. Approximately 2-3 ml of headspace was present. HCE (from a DMSO stock solution) was injected into each vial, using a syringe, to yield HCE concentrations of 7 and 3 ppm. Preliminary tests showed that the addition of 100 ppm yeast extract did not significantly increase the transformation rate, so yeast extract was not included in the rate study. Periodically, 2 ml of air was injected into the vial headspace and 2 ml of sample was removed, extracted with diethyl ether, and analyzed as discussed above. The purpose of the sealed vials was to prevent excessive HCE evaporation. The majority of the bacteria are expected to be facultative in nature.

Viable cell plate counts were made using Difco triptic soy broth agar under aerobic conditions and Difco thioglycollate agar under anaerobic conditions. Preliminary tests showed the anaerobic plate count number to be the

same as the aerobic counts. We therefore used the aerobic plate count number as the cell population to calculate the second-order rate constant.

## Results

Figure 14 shows plots of ln[HCE] versus time for initial HCE concentrations of 7 and 3 ppm and the control vial. The control vial yielded a pseudo-first order rate constant of 0.025 $hr^{-1}$, which was much slower than that of the vials containing cell suspensions. The plate counts for these experiments were: aerobic agar plates = 1.03 X $10^9$ CFU (colony forming unit) $ml^{-1}$, anaerobic agar plates = 1.21 X $10^9$ CFU $ml^{-1}$ at 0 hour; and aerobic agar plates = 1.35 X $10^9$ CFU $ml^{-1}$ from the 7 ppm vial and 1.26 X $10^9$ CFU $ml^{-1}$ from the three ppm vial.

The first- and second-order rate constants, microbial population, and HCE concentration are shown in Table 7.

Table 7

HCE First- and Second-Order Biotransformation Rate Constants Microbial Population, and HCE Concentrations

| [HCE] (ppm) | $k_b^1$ ($hr^{-1}$) | [X] (org $ml^{-1}$) | $k_{b2}$ (ml $org^{-1}hr^{-1}$) |
|---|---|---|---|
| 7 | 0.127 | $1.29 \times 10^9$ | $9.8 \times 10^{-11}$ |
| 3 | 0.199 | $1.29 \times 10^9$ | $1.5 \times 10^{-10}$ |

The average $k_{b_2}$ was $1.3 \times 10^{-10}$ ml $org^{-1}hr^{-1}$.

If a natural water body contains $1 \times 10^6$ org $ml^{-1}$, the expected pseudo-first-order rate constant will be

$$k_b^1 = (k_{b_2})(X) = (1.3 \times 10^{-10})(1 \times 10^6) = 1.3 \times 10^{-4}\ hr^{-1},$$

and the half-life will be

$$t_{1/2} = \ln 2/k_b^1 = 0.693/1.3 \times 10^{-2} = 5330\ hr \text{ or } 222\ days.$$

We therefore conclude that in aqueous systems of $1 \times 10^6$ org $ml^{-1}$ or less, the biotransformation of HCE will be a relatively slow process.

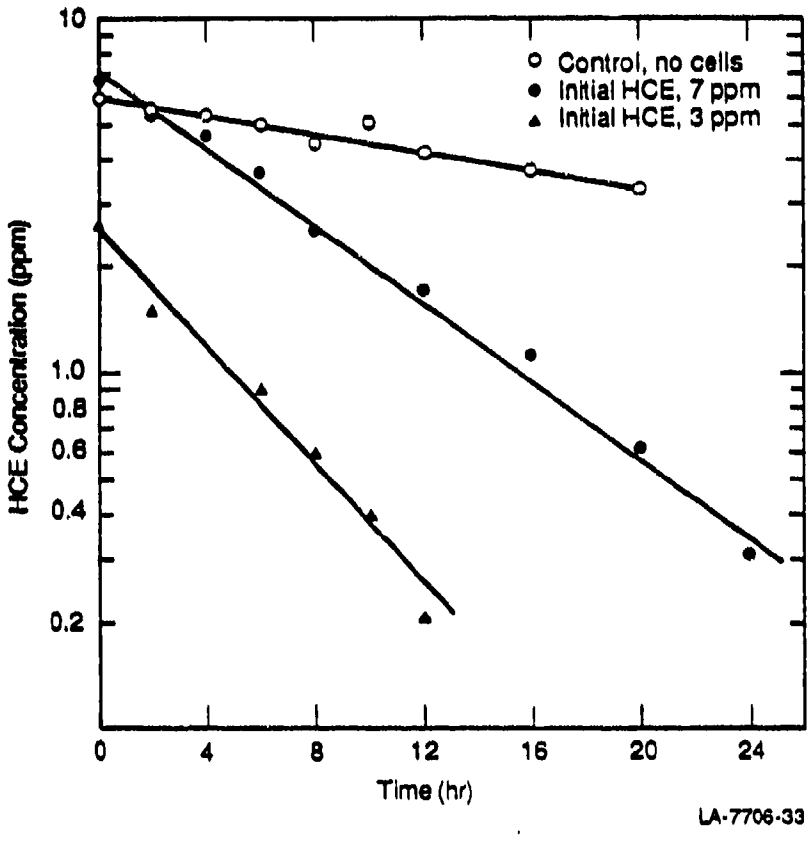


Figure 14. HCE BIOTRANSFORMATION IN HIGH-POPULATION CELL SUSPENSION

HCE Biotransformation Products

An examination of the gas chromatographic profiles of the HCE biotransformation showed the presence of two major metabolites (Figure 15). GC/MS analysis identified them as tetrachloroethylene and pentachloroethane. The identifications were confirmed by reference standards purchased from Aldrich Chemical Co. Retention times and mass spectra of the reference standards were identical to those of HCE metabolites. A small amount of trichloroethylene was also observed.

The formation of metabolites as a function of time and HCE concentration is shown in Figure 16; nearly 100% of the HCE is accounted for by tetrachloroethylene and pentachloroethane. The results suggest that the biotransformation occurs by two independent pathways. The major pathway is reduction, which yields tetrachloroethylene and the minor pathway is also reduction, which yields pentachloroethane (Scheme 5):

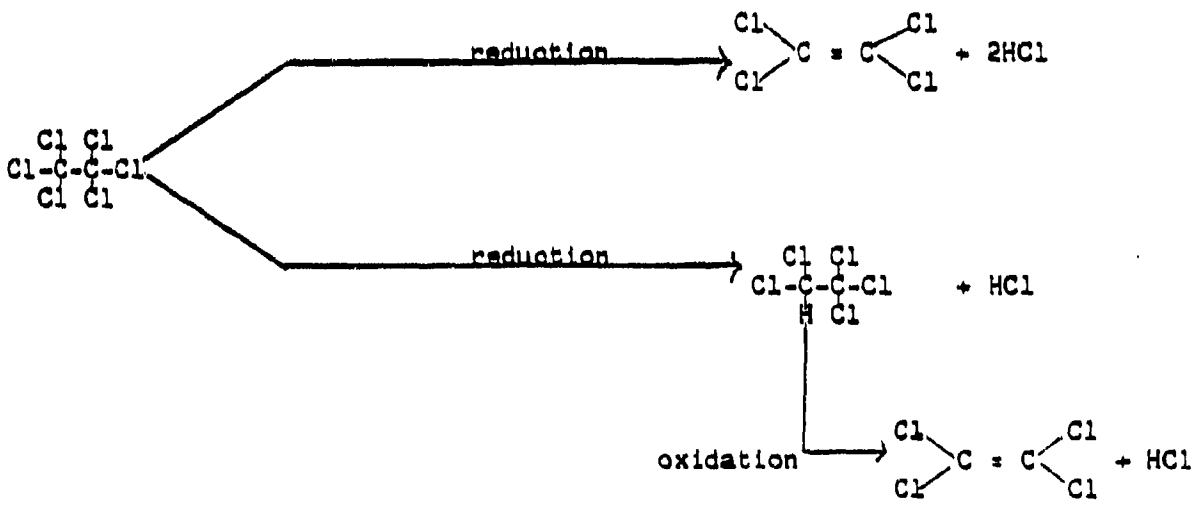


Scheme 5

Pentachloroethane can also eliminate HCl to produce more tetrachloroethylene.

It appears that after six hours, the major reductive pathway slows and the reductive pathway accelerates.

In the transformation of HCE we also observed the bioreduction of dimethylsulfoxide to dimethylsulfide (I) and dimethyldisulfide (II)

$$CH_3SCH_3 \longrightarrow CH_3SCH_3 + CH_3S\text{-}SCH_3$$

(I) (II)

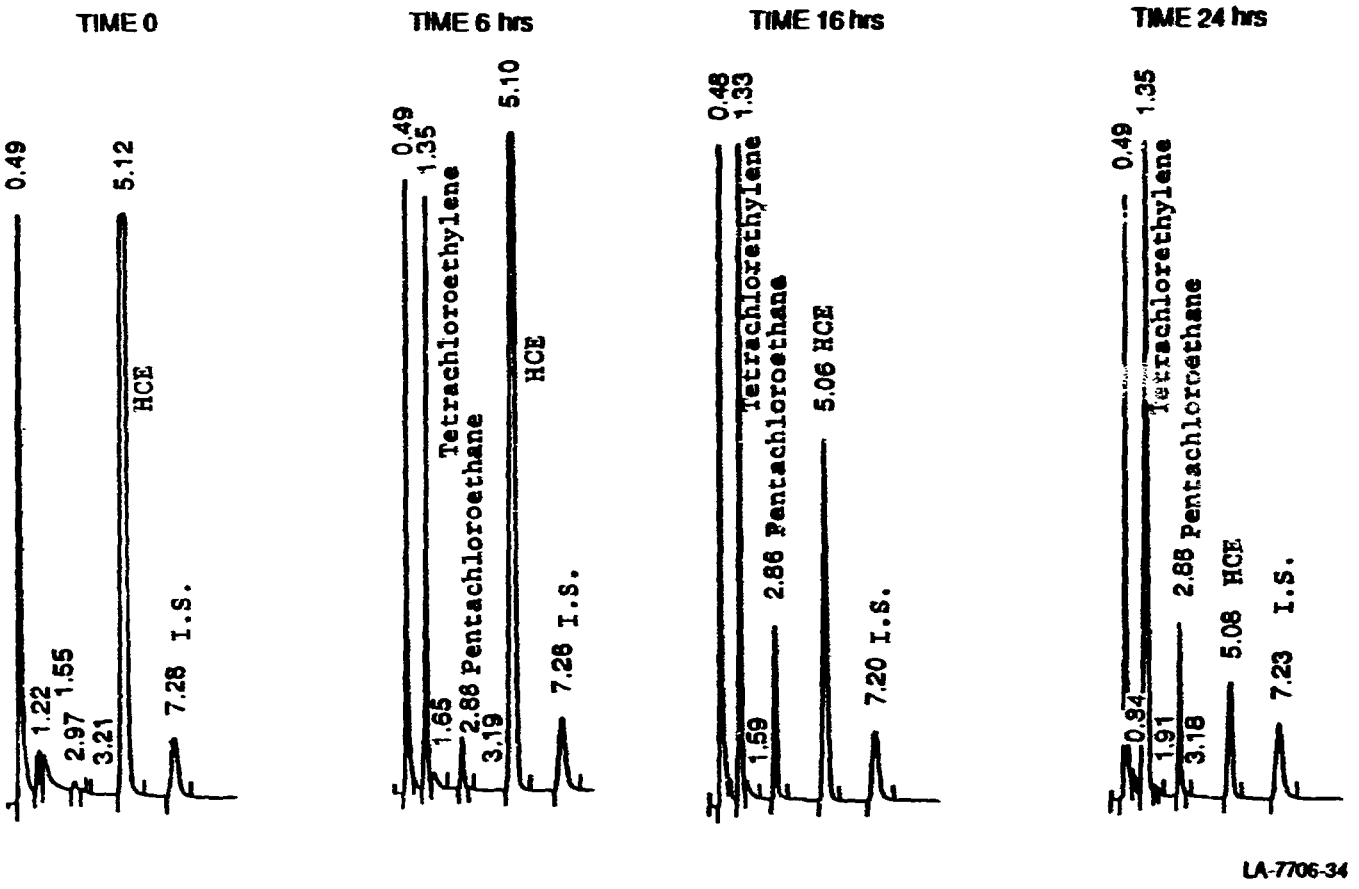


Figure 15. GC PROFILES OF HCE BIOTRANSFORMATION SAMPLE EXTRACTS AT 0, 6, 16, AND 24 HOURS

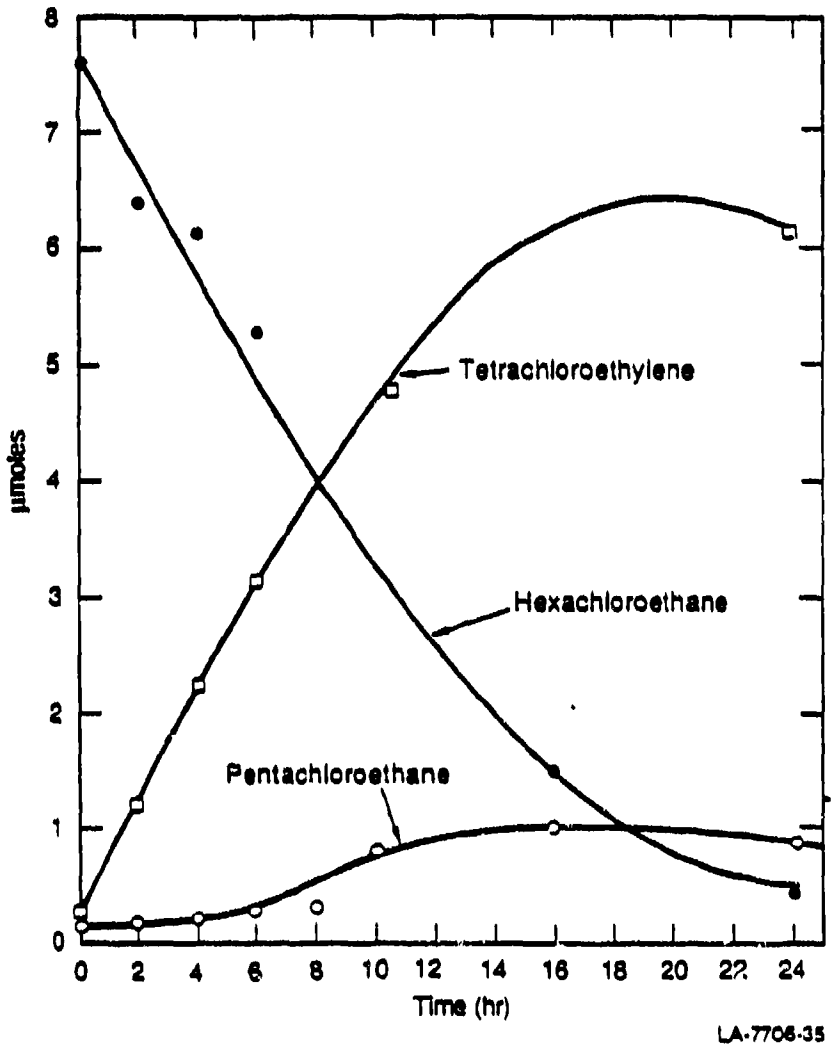


Figure 16. Loss of HCE and Formation of Metabolites

This transformation appears to be correlated to the transformation of HCE because each reaction is dependent on an electron source from other biological products (NADH, NADPH, flavin, flavoprotein, glulathione, etc.).

$$2e^- + 2H^+ + CH_3\overset{O}{S}CH_3 \longrightarrow CH_3SCH_3 + H_2O$$

$$2e^- + Cl_3CCCl_3 \longrightarrow Cl_2C{=}CCl_2 + 2Cl^-$$

$$2e^- + H^+ + Cl_3CCCl_3 \longrightarrow Cl_3CCHCl_2 + Cl^-$$

## Discussion

In Phase I, we established a volatilization rate constant, $k_v$, that was dependent on the mass transfer coefficient in the liquid phase ($k_v$) and the depth of the water body. For a lake or pond 180 deep, the $k_v$ value was 0.01 $hr^{-1}$ and the half-life was 70 hrs or 2.9 days. With a pseudo-first-order rate constant of $1.2 \times 10^{-4}$ hr, biotransformation would be 100 times slower than volatilization in the same lake or pond based on a normal cell count of $1 \times 10^6$ organisms $ml^{-1}$. If the organism concentration was increased 100 fold to $1 \times 10^8$ organisms $ml^{-1}$, the half-life from both processes would be competitive.

## Conclusions

The biotransformation of HCE in the environment will proceed with a first-order rate constant of approximately $1.2 \times 10^{-4}$ $hr^{-1}$. The rate of loss will not be significant unless organism populations reach $1 \times 10^8$ org $ml^{-1}$. The half-life at this organism population will be 2.2 days. The major products resulting from the biotransformation will be tetrachloroethylene and pentachloroethane.

## TASK 4

## Biotransformation of Nitroguanidine and Identification of Biotransformation Products

### Introduction

This study was undertaken to determine the rate constant for the biotransformation of nitroguanidine. It was determined from the Phase I study (Spanggord et al., 1985) that the biotransformation of NG could occur under both aerobic and anaerobic conditions, using organisms collected from NG holding ponds at Sunflower Army Ammunition Plant (SAAP). The biotransformation was shown to be a cometabolic process in which the organisms could degrade NG only in the presence of other organic nutrients (such as nutrient broth) and not as a sole carbon and energy source.

The initial biotransformations were performed in shaker flasks, using nutrient broth as a cosubstrate in natural waters collected from SAAP. When the flasks were returned to static conditions, the reaction rate became rapid. Under the static conditions, 90% of a 20 ppm NG solution containing 200 ppm nutrient broth and 1 g/L phosphate buffer was transformed in two days. It appears that under the static conditions, the microbes rapidly reduce the dissolved oxygen content, thereby creating a microaerophilic environment which appears to be the most favorable condition for NG to biotransform.

Because of the cometabolic nature of the biotransformation, the rate constant study was conducted using a high cell population of natural organisms acclimated to NG in nutrient broth. Since NG is not a growth nutrient, the Monod kinetic analysis cannot be applied. However, if the transformation is controlled by enzymes within the cell, the rate can be described as a pseudo-first-order rate expression (Equation 12).

$$\frac{dC}{dt} = - k_b^1 C \qquad \text{Eq. (12)}$$

where C is the concentration of NG and $k_b^1$ is the pseudo-first-order rate constant. This rate expression is applicable where the cell population remains at a constant level. Integration of Equation 12 yields Equation 13.

$$\ln C_o/C_t = k_b^1 t, \qquad \text{Eq. (13)}$$

where $C_o$ and $C_t$ are the concentration of NG at time zero and time t. By plotting lnC versus t, $k_b^1$ can be determined as the slope of the line by least-squares analysis. $k_b^1$ is a function of microbial population, X. Therefore, the second-order biotransformation rate constant, $k_{b_2}$, can be determined from Equation 14.

$$k_{b2} = k_b^1/[X], \qquad \text{Eq. (14)}$$

The determination of these rate constants was the objective of this study.

Methods

Microorganisms obtained from Pond B at SAAP were used in the kinetic study. Pond B water was collected by SAAP personnel on August 11, 1986 and shipped to SRI under ice by an overnight parcel carrier. To 250 ml of the Pond B water in a 500 ml erlenmeyer flask was added 1 g/L nutrient broth, 1 g/L yeast extract, 0.5 g/L potassium phosphate buffer (pH 7.0), and 10 ppm NG. The water was incubated at 20-25°C, with periodic shaking by hand. At various intervals, a 5-ml sample was removed, one drop of a 2% $HgCl_2$ solution was added to inhibit the enzymatic reaction, and the sample was analyzed by high-performance liquid chromatography (HPLC) using the following conditions.

Instrument: Hewlett-Packard 3500B liquid chromatograph

Column: 250 mm x 4.6 mm Zorbax C-8 (DuPont)

Solvent: Milli-Q water (100%)

Flow Rate: 0.8 ml/min

Detector: UV @ 254 nm

Retention Time: 5.31 min

Quantitation was achieved by the external standard method, using a standard calibration plot of nanograms of nitroguanidine versus peak area obtained from Hewlett-Packard 3390A digital integrator.

When more than 70% of NG was degraded, the microorganisms were transferred to a medium containing the same components as described above. After several transfers, the microorganisms were grown in deionized water medium containing 200 ppm nutrient broth, 200 ppm yeast extract, 0.5 g/L phosphate buffer, and 20 ppm NG solution in 1 liter contained in a 2-L flask loosely covered with aluminum foil and statically incubated. Typically, 90% of the NG was transformed in two days.

After two days of incubation, the broth was centrifuged at 4000 x G for 10 minutes, washed with phosphate buffer, and recentrifuged. The cells were resuspended in 250 ml of phosphate buffer to make a high population cell suspension, and 80 ml was dispensed into 150-ml bottles. NG was added to the bottles from an aqueous stock solution and incubated with or without the addition of nutrient broth (NB) and yeast extract (YE). Periodically, the bottles were shaken by hand and a 5 ml sample was removed, placed in a vial containing 1 drop of 2% $HgCl_2$ solution, and analyzed by HPLC. Viable cell counts were made with Difco triptic soy broth agar under aerobic conditions and with Difco fluid thioglycollate agar incubated in a BBL canopy pack microaerophilic system jar. The preliminary results showed nearly identical plate counts for the aerobic and microaerophilic plates, indicating that most of the bacteria are facultative.

## Results

Plots of lnC versus time appear in Figures 17 and 18 for NG at 2 ppm and 11 ppm with and without the presence of organic nutrients (NB and YE). The different NG concentration experiments were performed at different times and the experiments were performed over 10 hour periods. The initial aerobic plate count was used for the second-order biotransformation rate constant calculation. The plots clearly indicate the rate dependence on extra organic nutrients, which may serve as the energy source for the transformation and not just as growth substrates. The biotransformation by cells without additional nutrients may rely on stored energy to effect the transformation.

The first- and second-order rate constants determined for the biotransformation as a function of NG concentration and organic nutrient concentration are shown in Table 8.

Table 8

NG Biotransformation Rate Constants as a Function of NG and Nutrient Concentration

| [NG] (ppm) | [NB]+[YE] (ppm each) | $k_b^1$ ($hr^{-1}$) | [X] (org $ml^{-1}$) | $k_{b_2}$ (ml $org^{-1}hr^{-1}$) |
|---|---|---|---|---|
| 2.1 | 0 | 0.033 | $8.40 \times 10^7$ | $4.0 \times 10^{-10}$ |
| | 20 | 0.102 | " | $1.2 \times 10^{-9}$ |
| | 50 | 0.192 | " | $2.3 \times 10^{-9}$ |
| 8.5 | 0 | 0.078 | $1.67 \times 10^8$ | $4.6 \times 10^{-10}$ |
| | 20 | 0.303 | " | $1.8 \times 10^{-9}$ |
| | 50 | 0.341 | " | $2.0 \times 10^{-9}$ |
| 11.5 | 0 | 0.028 | $1.01 \times 10^8$ | $2.8 \times 10^{-10}$ |
| | 50 | 0.265 | " | $2.6 \times 10^{-9}$ |

The average second-order rate constant ($k_{b2}$) for microbes was 3.8 (± 0.9) x $10^{-10}$ ml $org^{-1}hr^{-1}$ without additional nutrients; 1.5 (± 0.4) x $10^{-9}$ ml $org^{-1}$ $hr^{-1}$ with 20 ppm nutrients; and 2.3 (± 0.3) x $10^{-9}$ ml $org^{-1}hr^{-1}$ with 50 ppm nutrients.

From the second-order rate constants it is possible to estimate NG persistence under specific environmental conditions. In a quiescent water containing 1 x $10^6$ org/ml and a low nutrient level, a first-order rate constant can be calculated and the half-life determined as shown in Equation 15 and 16.

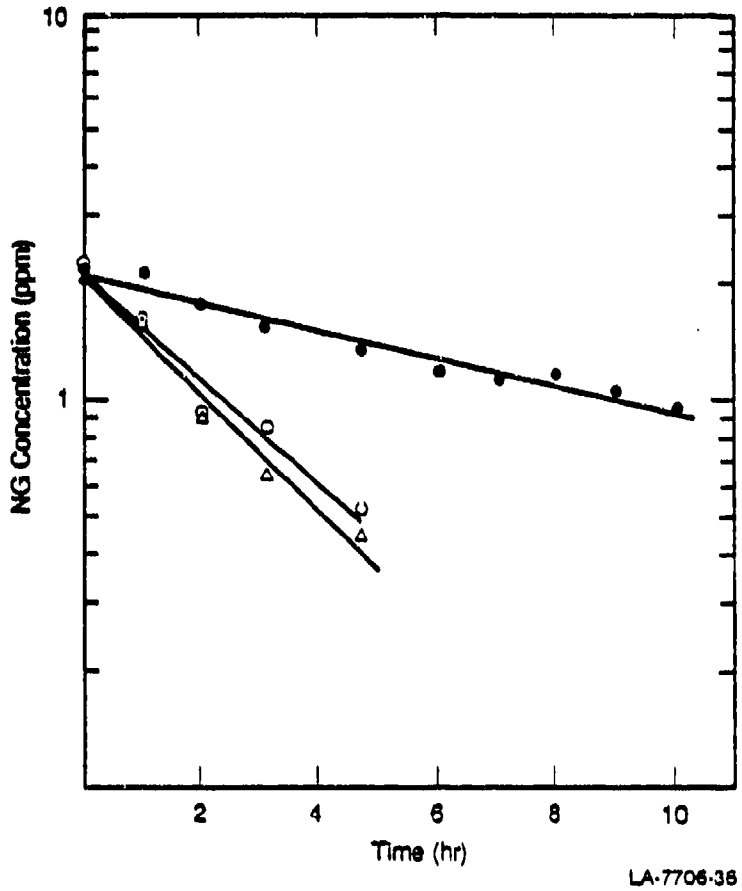


Figure 17. NG BIOTRANSFORMATION IN HIGH-POPULATION CELL SUSPENSION WITH INTIAL 2 ppm NG CONCENTRATION
- ● No NB or YE added
- ○ 20 ppm each of NB and YE added
- △ 50 ppm each of NB and YE added

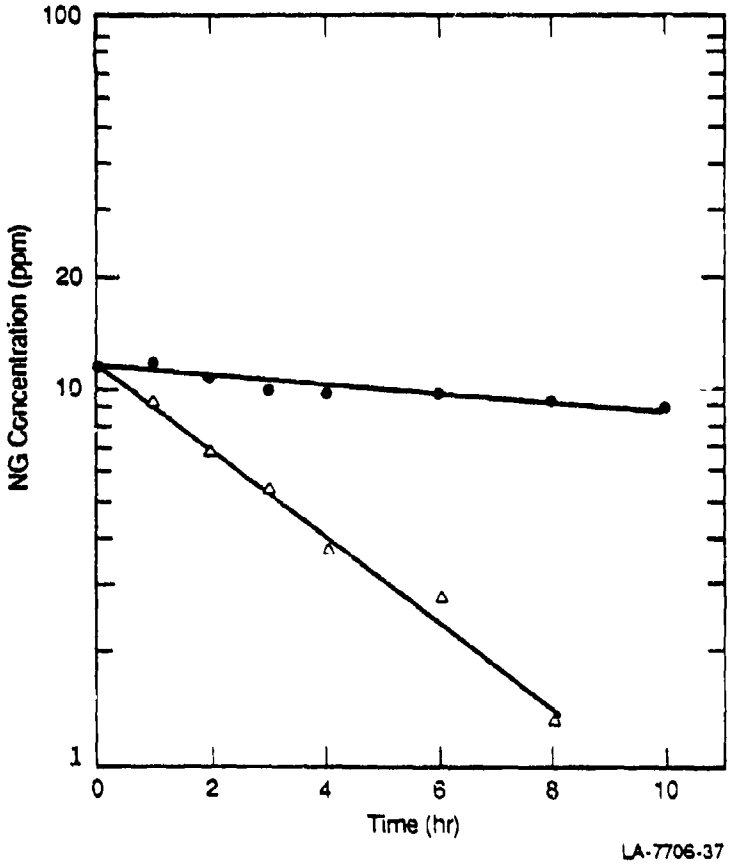


Figure 18. NG BIOTRANSFORMATION IN HIGH-POPULATION CELL SUSPENSION WITH INITIAL 11 ppm NG CONCENTRATION
- ● no NB or YE added
- ▲ 50 ppm each of NB and YE added

$$k_b^1 = (k_{b_2})(X) = (3.8 \times {}^{-10})(1 \times 10^6) = 3.8 \times 10^{-4} hr^{-1} \quad (15)$$

$$\text{half-life} = \ln 2/k_b^1 = 0.69/3.8 \times 10^{-4} = 2038 \text{ hr or } 85 \text{ days} \quad (16)$$

In a pond bottom containing decomposed organic matter, the microbial population may be in the range of $1 \times 10^7$ org/ml. Assuming 100 ppm organic matter, the first-order rate constant will be $[(2.3 \times 10^{-9}$ ml org$^{-1}$hr$^{-1}$) $(1 \times 10^7)]$ $2.3 \times 10^{-2} hr^{-1}$ and the half-life will be 30 hours.

NG Biotransformation Products

The monitoring of the NG biotransformation by HPLC indicated no new product formation that was resolvable and detectable at 254 nm. N-Nitrosoguanidine, an expected and resolvable transformation product, was not observed. We examined the aqueous phase for N-hydroxyguanidine under the conditions described for NG photolysis products but could not detect this component.

When the partially transformed solution was evaluated by ion chromatography in the anion mode, only traces of nitrate were observed that could be related to NG (Figure 19). In the cation mode, signals were observed for sodium, ammonium ion, and potassium, which are related to basal salts medium, and a long-eluting component of retention time (11.78 min) greater than that of hydroxyguanidine (10.07 min) or guanidine (10.29 min) (Figure 20). Possibly this component is aminoguanidine (I) resulting from the reduction of NG.

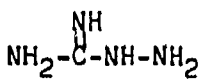

(I)

The aqueous suspension was centrifuged (2500 ppm for 10 min), filtered (0.45 μ), and lyophilized to a solid residue (principally inorganic salts). The residue was heated in the presence of 0.5 ml of BSTFA. The resulting extract was analyzed by GC/MS. The only product identified (as compared to reference spectra) was cyanamide (II) as the bis-trimethysilyl derivative (III).

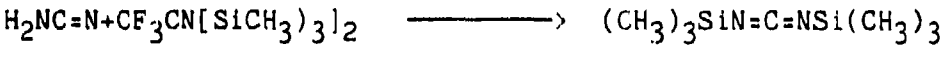

(II) (III)

Thus, these data suggest that cyanamide is one end product of NG biotransformation. The other nitrogen atoms of NG could be transformed to ammonia or nitrogen. A potential pathway for biotransformation is shown below.

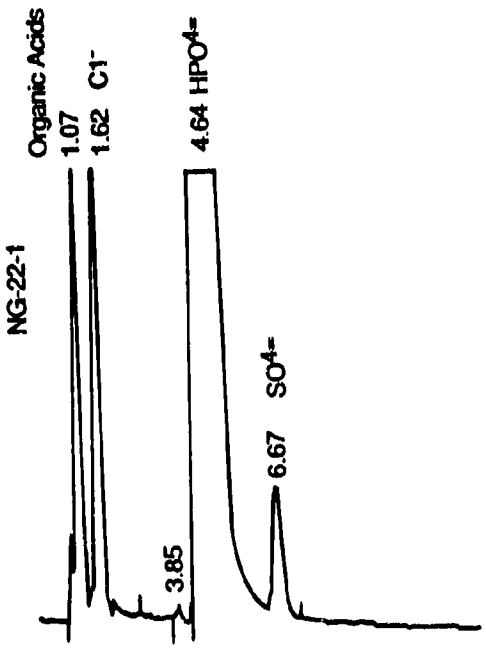


FIGURE 19. ANION CHROMATOGRAM OF BIOTRANSFORMED NG. TRACE LEVELS OF NITRATE OBSERVED AT 3.85 MINUTES

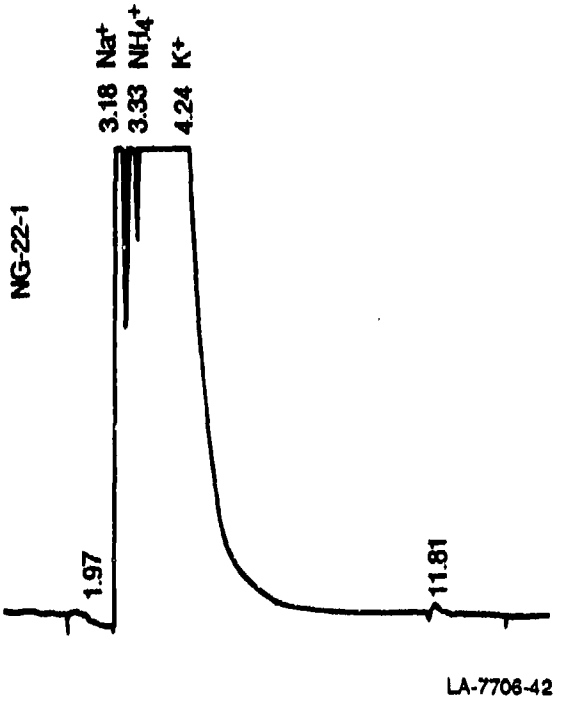


FIGURE 20 CATION CHROMATOGRAM OF BIOTRANSFORMED NG. GUANIDINE NITRATE AND HYDROXYGUANIDINE ELUTED AT 10.29 AND 10.05 MINUTES, RESPECTIVELY

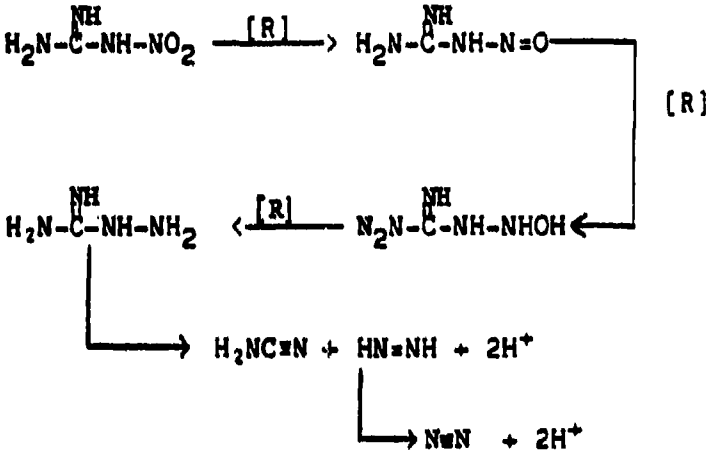


## Conclusions

Cyanamide appears to be an end product of NG utilization by microbes and there appears to be no build up of intermediate products that are detectable by GC, HPLC, or ion chromatography.

It is clear from this study that the microbial persistence of NG is dependent on the environment with regard to the oxygen and nutrient concentrations. To fully understand the relationship between the rate and these variables, a more detailed study is required. However, the measured rate constants should be useful as initial estimates of NG persistence in aquatic environments.

## TASK 5

## Biotransformation of Diethyleneglycol Dinitrate and Identification of Biotransformation Products

### Introduction

In our Phase I Study (Spanggord et al., 1985), diethyleneglycol dinitrate (DEGDN) was found to undergo biotransformation aerobically and anaerobically by microorganisms obtained from the Radford Army Ammunition Plant (RAAP). In this study we examined the biotransformation in more detail to derive pseudo-first-order and second-order biotransformation rate constants.

RAAP utilizes a bioreactor plant to treat munition wastes, including DEGDN, prior to discharge into the New River. We observed DEGDN to transform in a few days when added to freshly collected bioreactor effluent. The biotransformation appeared to be a cometabolic process, with ethanol serving as an effective cometabolic substrate. However, we found it difficult to maintain the viability of the organisms once the cosubstrates had been utilized. When the organisms from the bioreactor were transferred to basal salts medium containing DEGDN and ethanol, the biotransformation process was much slower. After several transfers, the half-life of transformation was more than a week in the presence of ethanol (200 ppm) and the results were not consistent. Under a microscope, we observed many protozoa in the mixed culture. It is possible that the protozoa prey on the DEGDN-utilizing bacteria and reduce the functional cell concentration. The viable cell count of the water, which was fed ethanol at 200 ppm several times, was only $10^7$ CFU (colony-forming units), which was much lower than expected. It appears from these results that other cosubstrates are important contributors to the biotransformation of DEGDN.

For the DEGDN biotransformation rate study, organisms from the RAAP bioreactor were grown in ethanol and basal salts medium containing DEGDN to produce a high-population cell suspension. Because of the cometabolic nature of the transformation, the microbes did not use DEGDN as a sole carbon source. Therefore, the widely used Monod kinetics is not applicable for determination of the biotransformation rate constant. However, if DEGDN biotransforms by the enzymes of the ethanol-grown cells, the loss of DEGDN can be described by a pseudo-first-order rate equation, as shown in Equation 17:

$$\frac{dC}{dt} = -k_b^1 C, \qquad (17)$$

where [C] is the concentration of DEGDN and $k_b^1$ is the pseudo-first-order rate constant. Integration of Equation (17) yields Equation (18)

$$\ln C_o/C_t = k_b^1 t \qquad (18)$$

where $C_o$ and $C_t$ are the concentration of DEGDN at time 0 and time t. By plotting lnC versus t, a straight line will result in slope $-k_b^1$.

Since $k_b^1$ is a function of microbial population (or enzyme concentration), the second-order rate constant $k_{b2}$ can be obtained by Equation 19.

$$k_{b2} = k_b^1/[X], \qquad (19)$$

where X is equal to the microbial population.

Methods

Microorganisms were obtained from the RAAP bioreactor plant effluent. The effluent was collected on July 2, 1986 and shipped to SRI in an ice-packed container. To the effluent were added 20 ppm of DEGDN and 200 ppm of ethanol. The sample was incubated at 25°C. Periodically, a 5 ml sample was withdrawn, 0.1 ml of 2% $HgCl_2$ solution was added to inhibit the enzyme reaction, and the DEGDN was analyzed by HPLC. The HPLC system employed a $C_{18}$ radial compression column (Waters Assoc.), and mobile phase of acetonitrile/water (50/50), and UV detection at 215 nm. Quantitation was achieved by the internal standard method using 3,5-dinitrotoluene as the internal standard.

After the DEGDN was more than half transformed, the medium broth was centrifuged at 4000 x G for 10 min, washed with 0.5 g/L phosphate buffer (pH 7.0), and centrifuged again. The cells were resuspended in 1/8 (run 1) or 1/20 (run 2) of the original volume of phosphate buffer to prepare a high population cell suspension for the biotransformation study. DEGDN was added to the cell suspension from an aqueous stock solution to yield a final concentration of 12 ppm with and without 100 ppm of ethanol as a substrate. Periodically, the cell suspension was shaken by hand and 4-ml samples were removed, quenched with 0.1 ml of 2% $HgCl_2$ solution, and analyzed for DEGDN by HPLC. Viable cell counts were made with Difco triptic soy broth agar after a series of dilutions of the sample.

Results

A plot of the ln $C_o/C_t$ versus time is shown in Figure 21 for Run 2 of two experiments. The transformation followed a straight line, indicating first-order kinetic behavior. Although ethanol was used for the growth of the biotransformation organisms, ethanol had little impact on the transformation rate, indicating that it is not required as an energy source to promote the DEGDN biotransformation.

The colony counts were relatively stable. For example in the Run 2 experiments, both suspension contained $4.7 \times 10^8$ CFU at day 0, $4.4 \times 10^8$ CFU at Day 1 and $5.0 \times 10^8$ CFU at Day 2. Therefore, the average of the three day's plate counts was used in the calculation.

Table 9 presents the pseudo-first-order and second-order rate constants and the microbial populations for two experiments performed in the presence and absence of ethanol.

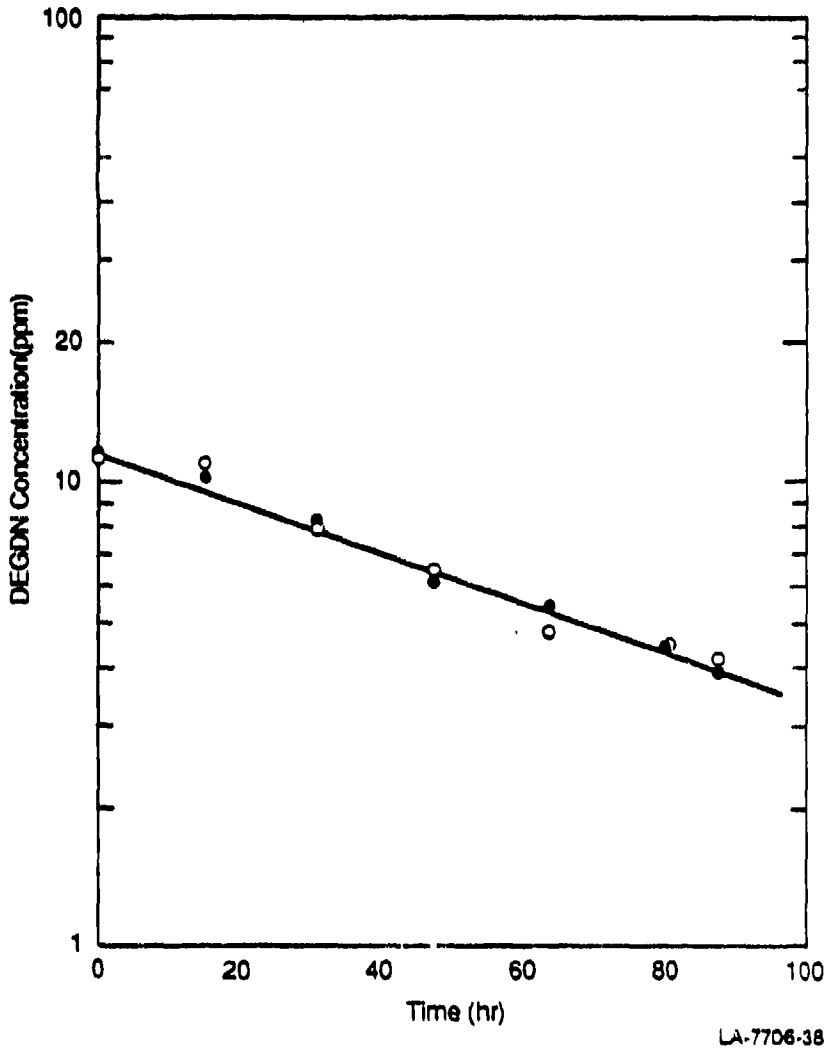


Figure 21. DEGDN BIOTRANSFORMATION IN HIGH CELL POPULATION WITH AND WITHOUT ETHANOL
- ● No ethanol added
- ○ 100 ppm ethanol added

Table 9

Rate Constants Determined For The Biotransformation of DEGDN

| Run No. | DEGDN (ppm) | Ethanol Added (ppm) | $k_b^1$ ($hr^{-1}$) | X (org $ml^{-1}$) | $k_{b2}$ (ml $org^{-1}hr^{-1}$) |
|---|---|---|---|---|---|
| 1 | 12 | 0 | 0.0077 | $1.44 \times 10^8$ | $5.3 \times 10^{-11}$ |
| 1 | 12 | 100 | 0.0097 | $1.97 \times 10^8$ | $4.9 \times 10^{-11}$ |
| 2 | 12 | 0 | 0.0125 | $4.70 \times 10^8$ | $2.7 \times 10^{-11}$ |
| 2 | 12 | 100 | 0.0127 | $4.70 \times 10^8$ | $2.7 \times 10^{-11}$ |

The average second-order rate constant for the four runs was 3.9 (± 1.4) x $10^{-11}$ ml $org^{-1}hr^{-1}$.

From the second-order rate constant it is possible to project DEGDN half-lives based on microbial populations. For example, in the bioreactor plant at RAAP with a microbial population of $10^{10}$ org/ml, the first-order rate constant would be

$$k_b^1 = k_{b_2} \times X = (3.9 \times 10^{-11} \text{ ml org}^{-1}\text{hr}^{-1})\ (1 \times 10^{10} \text{ org/ml})$$

$$k_b^1 = 0.39 \text{ hr}^{-1}$$

$$t_{1/2} = \ln 2/k_b^1 = 0.693/0.39 \text{ hr}^{-1} = 1.78 \text{ hr}$$

In a water body such as the New River with a microbial population of $1 \times 10^6$ org $ml^{-1}$, the half-life can be projected to be 17778 hr or 740 days. Thus, in the absence of the bioreactor or other cometabolic substrates, DEGDN is projected to be slowly biodegraded.

DEGDN Biotransformation Products

In following the biotransformation of DEGDN by HPLC, only one transformation product was observed as shown in Figure 22 for Run 2 without ethanol. The elution behavior of the product suggests that a higher polarity component than DEGDN (probably through enzymatic hydrolysis) is being generated; however, no metabolites were found to build up in the medium. A plot of the area response ratio of DEGDN and metabolite are shown in Figure 23. Also, nitrate and nitrite as measured by ion-exchange chromatography were not observed in the medium (<50ppb). Ammonia was observed to be present but ammonium salts are part of the basal salts medium, so ammonia could not be distinguished from that potentially arising from DEGDN.

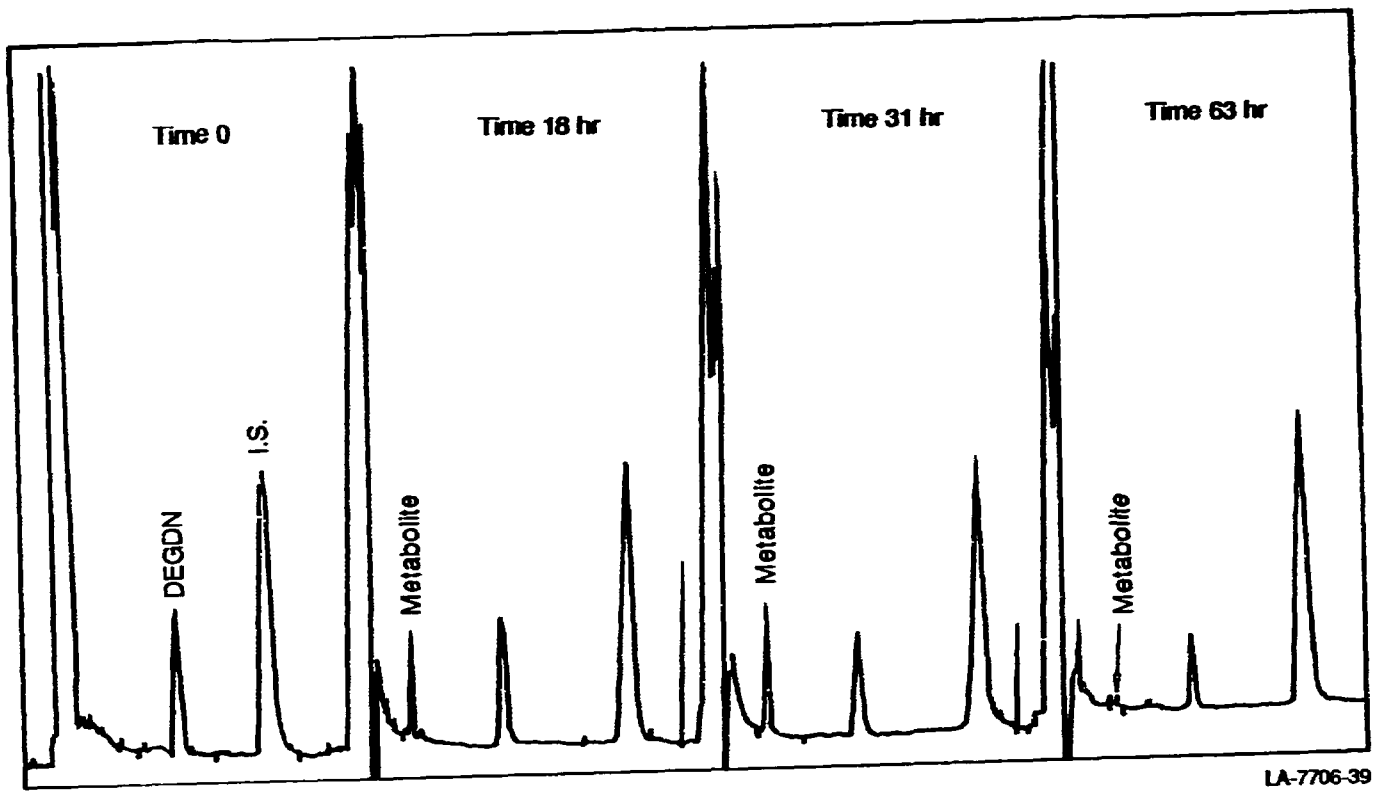


FIGURE 22. HPLC PROFILES OF DEGDN BIOTRANSFORMATION AND METABOLITE FORMATION

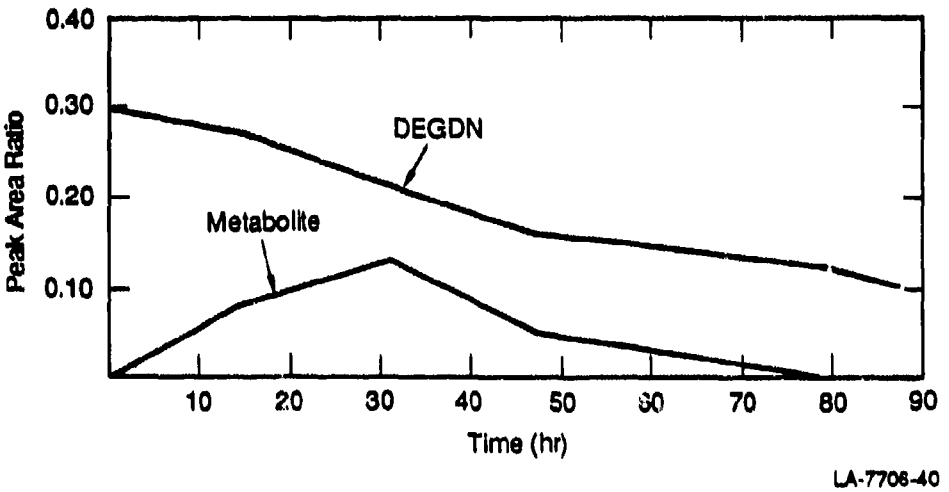


FIGURE 23 AREA RESPONSE RATIO VERSUS TIME FOR DEGDN AND METABOLITE RELATIVE TO THE INTERNAL STANDARD

The metabolite observed by HPLC was collected from the HPLC column by repetitive injections, combined, and concentrated by rotary evaporation.The concentrations were subjected to probe mass spectrometer analysis, but apparently sufficient concentrations were not available to generate interpretable spectra. Thus, because of the slow transformation rate and minor accumulation of products as observed by HPLC, product identifications could not be completed.

## Conclusions

The biotransformation of DEGDN was found to proceed with a second-order biotransformation rate constant of $3.9 \times 10^{-11}$ ml $org^{-1}hr^{-1}$. An environmental half-life of 740 days was projected in a water body such as the New River. Although the biotransformation of DEGDN proceeded readily in an organic rich environment (bioreactor), the HPLC profile of DEGDN and metabolites (at 215 nm) suggests that biotransformation products do not build up in the medium and are probably metabolized as carbon and energy sources.

## REFERENCES


Barthrop, J.A., Coyle, J.D. "Excited states in organic chemistry", New York; John Wiley & Sons. pp 311-314.

Berg, R., Becker, E. (1940). A new test for hydroxylamine by the formation of 5,8-quinolinequinone-5-(8-hydroxy-5-quinolylimide) designated "indooxine". Ber. 73B, 172-173. (Chem. Abstracts 34:3745).

Charton, M. (1965). The applicatin of the Hammett equation to amidines. J. Org. Chem. 30, 969-973.

Dennis, W. H. (1982). A memorandum report on the photolysis of nitroguanidine. SGRD-UBG-R, Sept. 29, 1982.

DeVries, J. E., Gantz, E. Spectrophotometric studies of dissociation constants of nitroguanidines, triazoles, and tetrazoles. (1954). J. Am. Chem. Soc. 76, 1008-1010.

Dulin, D., Mill, T. (1982). Development and evaluation of sunlight actinometers. Environ. Sci. Technol. 16, 815-820.

Edwards, J.O., Mueller, J.J. (1962). The rates of oxidation of nitrite ion by several peroxides. Inorg. Chem. 1, 696-699.

Federal Register (1985). Toxic substances control act test guidelines. 50 (188), pp 39285-39311, Sept. 27, 1985

Federal Register (1985). Toxic substances control act test guidelines. p 39293, Sept. 27, 1985

Haag, W.R., Hoigne, J. (1985). Photo-sensitized oxidation in natural water via OH radicals. Chemosphere 14, 1659-1671.

Haag, W.R., Hoigne, J. (1986). Singlet oxygen in suface waters - part III. photochemical formation and steady state concentrations in various types of waters. Environ. Sci. Technol. 20, 341-348.

Mill, T., Hendry, D.G., Richardson, H. (1980). Free-radical oxidants in natural waters. Science 207, 886-889.

Ovenberger, C.G., Anselme, J.P. (1963). A convenient synthesis of phenyldiazomethane. J. Am. Chem. Soc. 28, 592-593.

Sapse, A.M., Herzig, L., Snyder, G. (1981). A self-consistent field molecular orbital study of hydroxyguanidine. Cancer Res. 41, 1824-1828.

Spanggord, R.J., Chou, T.W., Mill, T., Podoll, R.T., Harper, J.C., Tse, D.S. (1985). Environmental fate of nitroguanidine, diethyleneglycol dinitrate, and hexachloroethane smoke - phase I. Final Report U.S. Army Medical Research and Development Command, Contract DAMD17-84-C-4252.

Walker, J.B. (1958). Role for pancreas in biosynthesis of creatinine. Proc. Soc. Exp. Biol. Med. 98, 7-9.

Zepp, R. G., Wolfe, N. L., Baughman, G. L., Hollis, R. C. (1977). Singlet oxygen in natural waters. Nature 267, 421-423.

DISTRIBUTION

25 copies
Commander
US Army Biomedical
Research and Development Laboratory
ATTN: SGRD-UBGM
Fort Detrick
Frederick, MD 21701-5010

1 copy
Commander
US Army Medical
Research and Development Command
ATTN: SGRD-RMI-S
Fort Detrick
Frederick, MD 21701-5012

2 copies
Defense Technical Information Center (DTIC)
ATTN: DTIC-DDA
Cameron Station
Alexandria, VA 22504-6145

1 copy
Dean
School of Medicine
Uniformed Services University of the
Health Sciences
4301 Jones Bridge Road
Bethesda, MD 20814-4799

1 copy
Commandant
Academy of Health Sciences, US Army
ATTN: AHS-CDM
Fort Sam Houston, TX 78234-6100

1 copy
Commander
US Army Bio Medical
Research and Development Laboratory
ATTN; SGRD-UBD-A/Librarian
Fort Detrick
Frederick, MD 21701-5010

1 copy
Commander
US Army Material Command
ATTN: AMCEN-A
5001 Eisenhower Ave.,
Alexandria, VA 22333-0001